

LU TP 14-22

DECOMPOSING COLOUR STRUCTURES INTO MULTIPLY BASES

Johan Thorén



LUNDS
UNIVERSITET

2014

Master's Thesis

Theoretical High Energy Physics
Department of Astronomy and Theoretical Physics
Lund University

Thesis advisor: *Malin Sjödaahl*

Abstract

In this thesis a method for decomposing QCD colour structures into multiplet bases is described. The method is applicable for any number of gluons and quarks. To achieve the decomposition requires the knowledge of group theoretical weights, so-called Wigner $3j$ and $6j$ coefficients. The number of required coefficients have been calculated for up to 12 external gluons, and been shown to scale well in the number of external partons. How to calculate the coefficients have been shown and for 6 external gluons they have been calculated.

Furthermore the colour structures of $N_g - 1$ basis vectors radiating a gluon have been decomposed into the N_g basis vectors. The viability of this has been examined for up to 10 external gluons by counting how many N_g basis vectors are projected on by the colour structures.

Contents

1	Introduction	1
2	Group theory for gluons	1
2.1	Group theory	2
2.1.1	Basic definitions in group theory	2
2.1.2	Special Unitary groups, $SU(N_c)$	3
2.1.3	Young diagrams and Dynkin indices	4
2.1.4	Young tableau multiplication	5
2.1.5	Diagrammatic notation	7
2.2	Colour space and bases	11
2.2.1	Projectors for $SU(N_c)$	12
2.2.2	Trace bases	13
2.2.3	Multiplet bases	14
2.3	Dynkin indices for arbitrary N_c	16
2.4	Young multiplication rules for $A \otimes M$	17
2.5	Generalisation to delimiter notation	20
2.6	Properties of the representations in $A^{\otimes n_g}$	22
2.6.1	First occurrence	22
2.6.2	Representations in $A^{\otimes n_g}$	23
3	Feynman diagrams in multiplet bases	26
3.1	Vacuum bubbles as sums over Wigner $3j$ and $6j$ coefficients	26
3.2	Example of decomposition	29
3.3	Representations and Wigner $6j$ coefficients	30
3.3.1	Wigner $3j$ and $6j$ coefficients	35
3.4	Required Wigner $6j$ coefficients and their symmetries	37
3.4.1	Counting the required Wigner coefficients	40
3.5	External Quarks	41
3.6	Evaluation of Wigner coefficients	43
4	Recursion relation colour structures in multiplet bases	45
4.1	Basis vector radiating gluon	46
4.2	Projection on basis vectors	49
5	Conclusions and outlook	49
	Appendices	51
A	Proof of finite sum formula for the partition function P	51
B	Basis vectors for 6 external gluons	52
C	Wigner coefficients for 6 external gluons	52

1 Introduction

In quantum field theories there is interference at the amplitude level, the contribution from different Feynman diagrams can enhance or cancel each other. For theories with Abelian gauge symmetries, for example Quantum Electrodynamics (QED), the gauge part of the Feynman diagrams correspond to numbers. For such theories the interference is a trivial addition of numbers. This is changed for theories with more complex symmetries, like Quantum Chromodynamics (QCD). For QCD the symmetry is non-Abelian, and the Feynman diagrams are now associated with vectors in a group vector space. Interference between Feynman diagrams now manifests itself as the interference of these vectors.

The high energy of the LHC leads to a high multiplicity of coloured particles in the perturbative regime of events. For the group theoretical part, this means that the vector space is large, making it computationally expensive to evaluate interferences. A systematic way of dealing with the vector space is by choosing a basis with some useful properties. Two commonly used types of bases are trace bases [1–9] and colour flow bases [10]. Both of these bases have some nice properties for gluon exchanges, gluon emission and recursion relations in the number of external gluons [1–10]. They do come with drawbacks though, the basis vectors are not orthogonal, and for a general QCD process they are not bases but rather spanning sets, i.e., the number of basis vectors is larger than the dimension of the vector space [3, 11]. One basis type that is orthogonal and minimal is the multiplet bases. Similarly to the trace and colour flow bases the vectors for the multiplet bases have the desirable property of being invariant under the symmetry group of QCD, $SU(3)$. Multiplet bases have so far been applied to amplitudes with few external legs [12–17], and recently a recipe for construction of the basis vectors for multiplet bases with any number of external particles has been found [11].

In this thesis the decomposition of colour structures into multiplet bases is explored. To this end, section 2 introduces some relevant group theory and a useful diagrammatic notation in section 2.1, the birdtrack notation. This notation is then applied for both trace bases and multiplet bases in section 2.2. The sections 2.3–2.6 introduce a notation for representations in $SU(N_c)$ and derive some useful results from that. In section 3 a method of decomposing colour structures into multiplet bases is introduced and applied to the colour structures associated with Feynman diagrams. Section 4 applies the same method for colour structures occurring in recursion relations in the number of external gluons.

2 Group theory for gluons

Group theory is the study of symmetries, which is invaluable for physics. Symmetries are especially important for particle physics, where the modern approach of constructing quantum field theories is to require the Lagrangian to be invariant under some local symmetry. In the standard model of particle physics the symmetries are $U(1)$, $SU(2)$ and $SU(3)$. The first two groups are the symmetries of the electroweak part of the theory and the last group is the symmetry group of the strong interactions, which this thesis will address.

This section starts by stating known results in group theory in sections 2.1-2.2, then a new notation for Young tableaux is introduced and applied in sections 2.3-2.6.

2.1 Group theory

In this section some basic definitions in group theory are presented, as well as some properties of the group relevant to the theory of strong interactions, QCD. The later subsections introduce Young tableaux, and their applications for this thesis, and a useful diagrammatic notation is defined and applied to a simple derivation.

2.1.1 Basic definitions in group theory

For this thesis some basic definitions of group theory are necessary. First the basis of group theory, the definition of a group. In physics it is often the representations of groups that are of interest, since a group is a collection of abstract objects, but a representation is a set of linear operators for which there exists many powerful mathematical tools. An important property of representations is also defined, their irreducibility. As the symmetry of interest is a continuous symmetry, the type of groups that deals with such symmetries, Lie groups, are defined as well.

Definition: a set of elements $g \in G$ with an associated operation, $*$, is called a group if they satisfy the four conditions:

- *Closure:* $\forall g_1, g_2 \in G, g_3 = g_1 * g_2 \in G$.
- *Associativity:* $\forall g_1, g_2, g_3 \in G : g_1 * (g_2 * g_3) = (g_1 * g_2) * g_3$.
- *Identity:* $\exists 1 : 1 * g = g * 1 = g, \forall g \in G$.
- *Inverse:* $\forall g \in G, \exists g^{-1} : g * g^{-1} = g^{-1} * g = 1$.

Groups are classified according to the commutativity of the operation $*$. If the operation is commutative, i.e. $\forall g_1, g_2 \in G : g_1 * g_2 = g_2 * g_1$, the group is called *Abelian*, otherwise, $(\exists g_1, g_2 \in G : g_1 * g_2 \neq g_2 * g_1)$ it is non-Abelian.

Definition: a mapping, D , of the elements of a group, G , onto linear operators is a representation if:

- The identity element, 1, of G is mapped onto the identity operator of the space the operators act on.
- It preserves the group multiplication laws, if $g_1, g_2 \in G, D(g_1 * g_2) = D(g_1)D(g_2)$.

If a representation, $D(g)$, can be put into a block-diagonal form for all group elements g by a change of basis, i.e.

$$S^{-1}D(g)S = \begin{pmatrix} D_1(g) & 0 & \dots \\ 0 & D_2(g) & \dots \\ \vdots & \vdots & \ddots \end{pmatrix} \quad (1)$$

it is reducible, if it is not reducible it is said to be irreducible.

Continuous groups for which the representation of a group element can be reached by repeatedly multiplying by infinitesimal group elements

$$D(\alpha) = 1 + i\alpha_a T^a + \mathcal{O}(\alpha^2), \quad (2)$$

are called Lie groups. Where α_a are infinitesimal parameters parametrising the deviation from the identity element. To fulfil the closure property of the group the generators must be closed, i.e. the multiplication of any two generators must be a sum of generators. This means that the commutator of any two generators can be written as

$$[T^a, T^b] = if_{abc}T^c. \quad (3)$$

Where f_{abc} are the structure constants of the group. The commutator of eq. (3) is called the Lie algebra of the group, and defines the group multiplication completely sufficiently close to the identity.

2.1.2 Special Unitary groups, $SU(N_c)$

The fundamental particles that interact strongly are the quarks and the gluons. These transform under irreducible representations of a Lie group, $SU(N_c)$ with $N_c = 3$. That this is the Lie group of QCD is well established, yet a common way of dealing with the group theoretic part of calculations in QCD with many external partons is to approximate N_c to be very large. This suppresses terms inversely proportional to N_c . It is therefore of interest to leave N_c as a free parameter, as this allows the results to be used for comparisons between the large N_c limit and $N_c = 3$ calculations.

The $SU(N_c)$ groups are the groups of transformations that leave invariant the scalar product of two vectors in a complex N_c -dimensional space (unitary) and the volume (special), $\epsilon^{\alpha_1\alpha_2\dots\alpha_{N_c}} q_{\alpha_1} q_{\alpha_2} \dots q_{\alpha_{N_c}}$. The type of transformations that fulfil this are rotations in a complex N_c -dimensional space. These features are ensured if the representations of the group elements are unitary, $UU^\dagger = 1$, and have $\det U = 1$. The group elements can be exponentially parametrised, $U = \exp(i\alpha_i T^i)$, where the T^i are called the generators of the group. Requiring the determinant of U to be 1, is equivalent to requiring the trace of the generators T^i to be 0.

For QCD the group $SU(3)$ is of interest since it can be shown to be the only simple group that has the delta function and the Levi-Civita tensor with three indices as primitive invariants [18]. A primitive invariant cannot be written as a linear combination of invariants without loops of lower rank. That the delta function and the Levi-Civita tensors are the primitive invariants mean that there are colour singlets constructed from a quark and an antiquark, and from $N_c = 3$ quarks (or 3 antiquarks).

If U is a representation of the group elements of a unitary group $U(N_c)$, then δ^α_β transforms as

$$\delta^\alpha_\beta \rightarrow U^\alpha_{\alpha'} U_\beta^{\beta'} \delta^{\alpha'}_{\beta'} = U^\alpha_{\alpha'} U_\beta^{\alpha'} = (UU^\dagger)^\alpha_\beta = \delta^\alpha_\beta. \quad (4)$$

If the determinant of the representations is also required to be 1, then the group is $SU(N_c)$, and the Levi-Civita tensor transforms as

$$\epsilon^{\alpha_1\alpha_2\dots\alpha_{N_c}} \rightarrow U^{\alpha'_1}_{\alpha_1} U^{\alpha'_2}_{\alpha_2} \dots U^{\alpha'_{N_c}}_{\alpha_{N_c}} \epsilon^{\alpha'_1\alpha'_2\dots\alpha'_{N_c}} = \det(U) \epsilon^{\alpha_1\alpha_2\dots\alpha_{N_c}} = \epsilon^{\alpha_1\alpha_2\dots\alpha_{N_c}}. \quad (5)$$

For $SU(N_c)$ there are three physically important irreducible representations, the fundamental, the anti-fundamental and the adjoint representations. The fundamental representation is the lowest dimensional faithful representation. A faithful representation is one where $D(g)$ for different g are distinct. The quarks in QCD transform under

the fundamental representation, it is a complex representation, so associated with it is an inequivalent representation (cannot be related by a simple unitary transformation) if $N_c > 2$, that the antiquarks transform under. The gluons of QCD transform under the adjoint representation.

2.1.3 Young diagrams and Dynkin indices

Irreducible representations of $SU(N_c)$ can be labeled by so-called Young tableaux [18–20]. A Young tableau is composed of n left-justified boxes, put into rows with a length that is equal or decreasing for each row reading downwards, with at most $N_c - 1$ rows. As an example consider

$$\begin{array}{|c|c|} \hline \square & \square \\ \hline \square & \\ \hline \end{array}, \quad (6)$$

corresponding to the adjoint representation for $SU(3)$. Young tableaux are very useful objects for group theoretical calculations. In this thesis they will be used for decomposing tensor products of irreducible representations into direct sums of irreducible representations and for calculating the dimension of the representations. In section 2.2.1 another use of them will be mentioned.

Instead of drawing the boxes one can denote the Young tableaux, and hence the irreducible representations of $SU(N_c)$, by $N_c - 1$ numbers. One way of denoting a Young tableau is by the $N_c - 1$ numbers, α_i , $i = 1, \dots, N_c - 1$, being the number of columns of length i [18, 20]. These numbers are called the Dynkin indices of the Young tableau. An example is $(2, 1, 1)$ in $SU(4)$

$$(2, 1, 1) = \begin{array}{cccc} \overbrace{\square}^1 & \overbrace{\square}^1 & \overbrace{\square \square}^2 & \\ \square & \square & \square & \\ \square & & & \\ \square & & & \end{array}. \quad (7)$$

The dimension of the $SU(N_c)$ representation, α , associated with a Young tableau given by the Dynkin indices $(\alpha_1, \dots, \alpha_{N_c-1})$ can be calculated from the Young tableau [18, 20]. This is done in two steps, the first is finding the polynomial $f_Y(N_c)$ given by placing N_c in the box in the first row and column, the remaining boxes are filled with numbers such that the following conditions are fulfilled

- The numbers increase by 1 per box reading left to right along a row.
- Reading downwards along a column the numbers decrease by 1 per box.

The polynomial is now formed by taking the product of all of the numbers in the boxes. Using eq. (6) as an example, the numbers are filled in as

$$\begin{array}{|c|c|} \hline N_c & N_c+1 \\ \hline N_c-1 & \\ \hline \end{array} \Rightarrow f_Y(N_c) = N_c(N_c - 1)(N_c + 1). \quad (8)$$

The second part is calculating a number, $|Y|$, using the so-called hook rule. Similarly to the previous step all of the boxes are filled with numbers, then the product of them

is taken to be $|Y|$. For this the numbers are given by the number of boxes below and to the right of the box of interest, plus one from the box itself. For the above example this gives

$$\begin{array}{|c|c|} \hline 3 & 1 \\ \hline 1 & \\ \hline \end{array} \Rightarrow |Y| = 3. \quad (9)$$

Finally the dimension is given by

$$d_\alpha = \frac{f_Y(N_c)}{3}. \quad (10)$$

For our example the dimension is $d_\alpha = \frac{1}{3}N_c(N_c - 1)(N_c + 1)$, for $N_c = 3$ this is 8, as expected for the adjoint representation.

The representations of $SU(N_c)$ have associated with them a conjugate representation. If this is related by a unitary transformation then the representation is real, otherwise it is complex and the two representations are inequivalent. If the Young tableau for a representation α has the Dynkin indices $(\alpha_1, \dots, \alpha_{N_c})$, then the conjugate representation of α , $\bar{\alpha}$ has the Dynkin indices $(\alpha_{N_c}, \dots, \alpha_1)$. In terms of the Young tableau, one first adds boxes (here denoted \blacksquare , to distinguish them from the original boxes) until all columns that had at least 1 box are of length N_c . As an example, consider $(2, 1, 1)$ for $SU(4)$, adding the boxes gives

$$\begin{array}{|c|c|c|c|} \hline & & & \\ \hline & & & \\ \hline & & \bullet & \bullet \\ \hline & \bullet & \bullet & \bullet \\ \hline \bullet & \bullet & \bullet & \bullet \\ \hline \end{array}. \quad (11)$$

The original boxes are now removed, and the new boxes are rotated 180° . The markings are removed and the result is the Young tableau of the conjugate representation

$$\begin{array}{|c|c|c|c|} \hline & & & \\ \hline & & & \\ \hline & & & \\ \hline & & & \\ \hline & & & \\ \hline \end{array}. \quad (12)$$

Note that it has the Dynkin indices $(1, 1, 2)$ as it should. The representations for which this gives back the original Young tableau are real representations, one example is the adjoint representation.

2.1.4 Young tableau multiplication

Decomposing a tensor product for $SU(N_c)$ can be done with Young tableaux by a simple algorithm, for proof see [19]. The rules will be stated here along with an $SU(3)$ example. First the Young diagrams of the two representations are drawn, the example tensor product will be $15 \otimes 8$ of $SU(3)$,

$$\begin{array}{c} 15 \\ \begin{array}{|c|c|c|} \hline & & \\ \hline & & \\ \hline & & \\ \hline \end{array} \\ (2, 1) \end{array} \otimes \begin{array}{c} 8 \\ \begin{array}{|c|c|} \hline & \\ \hline & \\ \hline & \\ \hline \end{array} \\ (1, 1) \end{array}. \quad (13)$$

The two representations have been denoted in three ways, as the dimension of the representations in $SU(3)$ (from eq. (10)), as Young diagrams and with Dynkin indices. The first step is to add letters to the boxes of one of the diagrams, as for the first row, bs for the second, and so on,

$$\begin{array}{|c|c|c|} \hline & & \\ \hline & & \\ \hline \end{array} \otimes \begin{array}{|c|c|} \hline a & a \\ \hline b & \\ \hline \end{array}. \quad (14)$$

Now the boxes labeled a are added to the unlabelled diagram, to create tableaux fulfilling the following three criteria:

- (i) The number of boxes in the rows are weakly decreasing going downwards.
- (ii) No column contains more than one a (or b , or c, \dots).
- (iii) No column is longer than N_c .

For eq. (14) this step gives

$$\begin{array}{|c|c|c|} \hline & & \\ \hline & & \\ \hline \end{array} \otimes \begin{array}{|c|c|} \hline a & a \\ \hline b & \\ \hline \end{array} \rightarrow \begin{array}{|c|c|c|c|} \hline & & a & a \\ \hline & & & \\ \hline \end{array} \oplus \begin{array}{|c|c|c|} \hline & & a \\ \hline & & \\ \hline \end{array} \oplus \begin{array}{|c|c|c|c|} \hline & & & a \\ \hline & & & \\ \hline \end{array} \oplus \begin{array}{|c|c|c|} \hline & & \\ \hline & a & a \\ \hline \end{array} \oplus \begin{array}{|c|c|c|} \hline & & \\ \hline & a & \\ \hline \end{array}. \quad (15)$$

The next step is to repeat this procedure for the boxes labeled b on the tableau from the previous step. Again the resulting tableaux should fulfil the three conditions, (i), (ii) and (iii), above, and an additional condition:

- (iv) Reading from right to left, and going downwards the sequence of letters is admissible, meaning that at no point in the sequence there are more bs than as (or more cs than bs , etc.).

Performing this step for the first term of eq. (15) gives

$$\begin{array}{|c|c|c|c|} \hline & & a & a \\ \hline & & & \\ \hline \end{array} \rightarrow \begin{array}{|c|c|c|c|} \hline & & a & a \\ \hline & & b & \\ \hline \end{array} \oplus \begin{array}{|c|c|c|c|} \hline & & & a \\ \hline & & & \\ \hline \end{array}. \quad (16)$$

Here is an example of the application of condition (iv), the tableau:

$$\begin{array}{|c|c|c|c|c|} \hline & & & a & a & b \\ \hline & & & & & \\ \hline \end{array},$$

has an inadmissible sequence, baa , so it is not allowed. Similarly the other four terms of eq. (15) give

$$\begin{array}{|c|c|c|c|} \hline & & & a \\ \hline & & & \\ \hline \end{array} \rightarrow \begin{array}{|c|c|c|c|} \hline & & & a \\ \hline & & a & b \\ \hline \end{array} \oplus \begin{array}{|c|c|c|c|} \hline & & & a \\ \hline & & & \\ \hline \end{array},$$

$$\begin{array}{|c|c|c|c|} \hline & & & a \\ \hline & & & \\ \hline \end{array} \rightarrow \begin{array}{|c|c|c|c|} \hline & & & a \\ \hline & & b & \\ \hline \end{array},$$

$$\begin{array}{ccc}
\begin{array}{|c|c|c|} \hline & & \\ \hline a & a & \\ \hline \end{array} & \rightarrow & \begin{array}{|c|c|c|} \hline & & \\ \hline & a & a \\ \hline b & & \\ \hline \end{array}, \\
\\
\begin{array}{|c|c|c|} \hline & & \\ \hline & a & \\ \hline a & & \\ \hline \end{array} & \rightarrow & \begin{array}{|c|c|c|} \hline & & \\ \hline & a & \\ \hline a & b & \\ \hline \end{array}.
\end{array} \tag{17}$$

If there were more rows in the labeled tableau the same procedure as for b would be repeated for c , and d , and so on. The final two steps before arriving at the result are to remove the letters and to remove all columns with length N_c , as they correspond to the same representation as the diagram without those column. An example of this is

$$\begin{array}{|c|c|c|} \hline & & \\ \hline & & \\ \hline & & \\ \hline \end{array} = \begin{array}{|c|} \hline \\ \hline \end{array},$$

for $N_c = 3$. Adding together the results of eq. (16) and (17) gives the decomposition of the tensor product in eq. (13),

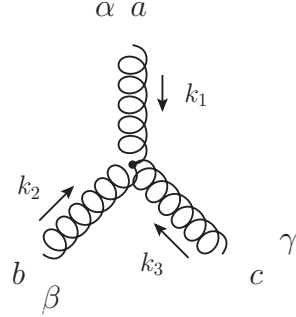
$$\begin{array}{c}
\begin{array}{|c|c|c|} \hline & & \\ \hline & & \\ \hline \end{array} \otimes \begin{array}{|c|c|} \hline & \\ \hline & \\ \hline \end{array} = \\
\begin{array}{|c|c|} \hline & \\ \hline & \\ \hline \end{array} \quad \begin{array}{|c|c|} \hline & \\ \hline & \\ \hline \end{array} \\
(2,1) \quad (1,1) \\
= \\
\begin{array}{|c|c|c|c|} \hline & & & \\ \hline & & & \\ \hline \end{array} \oplus \begin{array}{|c|c|c|} \hline & & \\ \hline & & \\ \hline \end{array} \oplus \begin{array}{|c|c|c|} \hline & & \\ \hline & & \\ \hline & & \\ \hline \end{array} \oplus \begin{array}{|c|c|c|} \hline & & \\ \hline & & \\ \hline & & \\ \hline \end{array} \oplus \begin{array}{|c|c|c|} \hline & & \\ \hline & & \\ \hline & & \\ \hline \end{array} \oplus \begin{array}{|c|c|} \hline & \\ \hline & \\ \hline \end{array} \oplus \begin{array}{|c|} \hline \\ \hline \end{array}. \tag{18} \\
(3,2) \quad (4,0) \quad (1,3) \quad (2,1) \quad (2,1) \quad (0,2) \quad (1,0)
\end{array}$$

The dimensions can be used as an extra check that the decomposition is correct. Since the representations on the right side should span the entire space of the tensor product the dimensions must be the same on both sides. For our example $15 \cdot 8 = 120$, and $42 + 15 + 24 + 15 + 15 + 6 + 3 = 120$.

2.1.5 Diagrammatic notation

Group theoretic calculations can be performed diagrammatically by so-called birdtracks [18], instead of with tensor indices. Similar to Feynman diagrams one has propagators, corresponding to delta functions in representations and their indices, and vertices, tensors connecting three representations. The difference to Feynman diagrams is that the calculations are actually performed entirely in this notation, it is not just a mnemonic device for finding the mathematical expression.

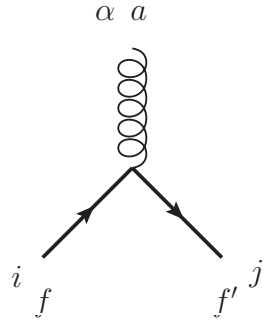
The relevant Feynman rules for QCD are



$$= g f_{abc} \left[g^{\alpha\beta} (k_1 - k_2)^\gamma + g^{\beta\gamma} (k_2 - k_3)^\alpha + g^{\gamma\alpha} (k_3 - k_1)^\beta \right]$$

(19)

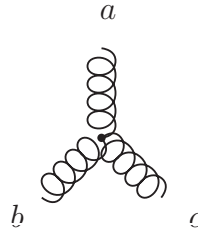
and



$$= i g \gamma^\alpha \delta_f^{f'} (T^a)^i_j.$$

(20)

Where the greek letters are four-vector indices, a , b and c are adjoint representation indices, i and j are antiquark and quark indices, f and f' are flavour indices and the k s are four-momenta. This report will only deal with the colour structure, so henceforth all vertices will only denote the colour part, i.e.



$$= i f_{abc}$$

(21)

Where there can be any number of legs, having just one leg on the right side of X in eq. (34) is only to make it clearer. With this the scalar product, eq. (33), in diagrammatic notation is

$$\langle \mathbf{X} | \mathbf{Y} \rangle = \text{Diagram} \quad . \quad (35)$$

2.2.1 Projectors for $SU(N_c)$

Projection operators, P , are linear transformations from a vector space into itself that are idempotent, meaning that

$$P^2 = P. \quad (36)$$

These operators project onto a subspace of the entire vector space, the set of projection operators that will be of interest here project onto transversal subspaces, i.e.

$$P_i P_j = \delta_{ij} P_i. \quad (37)$$

They should also fulfil a completeness relation, i.e. that the sum of all of the subspaces is the entire vector space, i.e.

$$1 = \sum_i P_i. \quad (38)$$

For the multiplet bases the projection operators of interest are those that project onto subspaces that transform under irreducible representations. The projector P_α should be invariant under the group action of the representation it projects onto, $D_\alpha(g)$, for all g , i.e.

$$D_\alpha^{-1}(g) P_\alpha D_\alpha(g) = P_\alpha, \quad \forall g \in G \quad (39)$$

$$\Rightarrow P_\alpha D_\alpha(g) = D_\alpha(g) P_\alpha, \quad \forall g \in G. \quad (40)$$

From Schur's lemma, eq. (24), P_α must be proportional to the identity matrix for the space spanned by $D_\alpha(g)$, which by definition has the dimension of the representation D_α . Using the idempotency of the projector, eq. (36), the scale factor in Schur's lemma is determined to be 1. The projector is then the identity operator in the space, so that its trace is the dimension of this space, which is the dimension of the representation D_α , hence

$$\text{Tr } P_\alpha = d_\alpha. \quad (41)$$

In [11] a method of constructing the projection operators for the irreducible representations of $A^{\otimes n_g}$ is presented. For this report these will be of use in evaluating the weights for a given colour structure on the multiplet basis vectors. From Young tableaux so-called Young projectors can be constructed. Each box in the Young tableau correspond to a quark index, these indices are symmetrized along the rows and anti-symmetrized along the columns. As an example, one of the Young projectors (the

numbers in the boxes could be assigned with 2 and 3 interchanged) for the adjoint representation in $SU(3)$ in $q \otimes q \otimes q$ is

$$\begin{array}{|c|c|} \hline 1 & 2 \\ \hline 3 & \\ \hline \end{array} \rightarrow \begin{array}{c} \rightarrow \rightarrow \rightarrow \\ \rightarrow \rightarrow \rightarrow \\ \rightarrow \rightarrow \rightarrow \end{array} \begin{array}{c} \text{white box} \\ \text{black box} \end{array} \begin{array}{c} \rightarrow \rightarrow \rightarrow \\ \rightarrow \rightarrow \rightarrow \\ \rightarrow \rightarrow \rightarrow \end{array} . \quad (42)$$

The white box is a symmetrizer, it is the sum of all permutations of the n indices entering it, multiplied by a combinatorial factor of $1/n!$. Similarly the black box is an antisymmetrizer, it is a sum of the permutations of the n indices, but with a minus sign in front of the permutations that take an odd number of index interchanges to arrive at from the identity permutation.

2.2.2 Trace bases

For comparison it is of interest to examine a commonly used [1–9] type of basis, the trace bases. This requires the Fierz identity, which is just a simple rewriting of the completeness relation, eq. (23), for a quark and an antiquark. With μ being the fundamental representation and ν the conjugate of the fundamental representation, the completeness relation gives (since $q \otimes \bar{q} = 1 \oplus A$, so $\alpha = 1, A$)

$$\begin{array}{c} \rightarrow \rightarrow \\ \leftarrow \leftarrow \end{array} = \frac{d_1}{\text{loop}} \begin{array}{c} \rightarrow \\ \leftarrow \end{array} \begin{array}{c} \leftarrow \\ \rightarrow \end{array} + \frac{d_A}{\text{loop}} \begin{array}{c} \rightarrow \\ \leftarrow \end{array} \begin{array}{c} \leftarrow \\ \rightarrow \end{array} \begin{array}{c} \text{loop} \\ \text{loop} \end{array} \begin{array}{c} \leftarrow \\ \rightarrow \end{array} . \quad (43)$$

For the first term a specific normalisation has been picked for the quark-antiquark-singlet vertex, i.e.

$$\begin{array}{c} \rightarrow \\ \leftarrow \end{array} \begin{array}{c} \leftarrow \\ \rightarrow \end{array} \begin{array}{c} \text{double line} \\ \text{double line} \end{array} \begin{array}{c} \rightarrow \\ \leftarrow \end{array} = \begin{array}{c} \leftarrow \\ \rightarrow \end{array} . \quad (44)$$

As for eq. (30) one can pick any normalisation for this vertex, since it cancels (there are two such vertices in the numerator and two in the denominator). Clebsch-Gordan coefficients are normalised such that the weights in the completeness relation, eq. (23), are 1 for all α . This is not desirable here, since it is not symmetric in the legs of the vertices. With such a normalisation, different instances of the vertices between α , β and γ would be normalised differently, depending on whether they were μ , ν or α in the completeness relation, eq. (23). A loop of a representation, such as in the factor of the first term in eq. (43), is just the dimension of the representation (it is an internal line so its index is summed over). Using this and that the dimension of the singlet is 1, gives a factor of $1/N_c$ for the first term of eq. (43). With the normalisation defined by eq. (30) the factor in front of the second term is $1/T_R$. Now eq. (43) can be reorganising to give the Fierz identity,

$$\begin{array}{c} \rightarrow \\ \leftarrow \end{array} \begin{array}{c} \leftarrow \\ \rightarrow \end{array} \begin{array}{c} \text{loop} \\ \text{loop} \end{array} \begin{array}{c} \leftarrow \\ \rightarrow \end{array} = T_R \left(\begin{array}{c} \rightarrow \rightarrow \\ \leftarrow \leftarrow \end{array} - \frac{1}{N_c} \begin{array}{c} \rightarrow \\ \leftarrow \end{array} \begin{array}{c} \leftarrow \\ \rightarrow \end{array} \right) \begin{array}{c} \leftarrow \\ \rightarrow \end{array} . \quad (45)$$

The decomposition into the trace bases is done by three substitution rules

1. The four-gluon vertices are removed by

$$\text{Four-gluon vertex} = \text{Four-gluon vertex with horizontal internal line} + \text{Four-gluon vertex with vertical internal line} + \text{Four-gluon vertex with diagonal internal line} \quad (46)$$

2. The three-gluon vertices are rewritten in terms of the fundamental representation by use of eq. (31).
3. Any internal gluons are removed by the Fierz identity, eq. (45).

An example of the trace bases for an amplitude with 7 external gluons and one external quark-antiquark pair is

$$\text{Grey blob with 7 gluons and 1 quark-antiquark pair} = A_1 \text{ (3 vertical gluons, 1 quark-antiquark pair)} + A_2 \text{ (3 vertical gluons, 4-gluon vertex, 1 quark-antiquark pair)} + \dots \quad (47)$$

where A_1, A_2, \dots are weights depending on how the external particles are connected inside the grey blob. It is referred to as trace bases due to the form of the final expression as in eq. (47), the terms are closed or open quark lines with attached gluons, if they are closed they correspond to traces over generators.

A problem with this basis is that it is over-complete if $N_g > N_c$, with the number of spanning vectors being $\text{Subfactorial}(N_g) \approx N_g!/e$ [3, 11]. These types of bases are also non-orthogonal under the scalar product of eq. (35), making it hard to deal with many external gluons, due to having to evaluate $\sim (N_g!/e)^2$ terms.

2.2.3 Multiplet bases

A minimal and orthogonal basis is of interest, to reduce the number of basis vectors (minimality) and making squaring trivial (orthogonality). Another desirable property of the bases are that the basis vectors should be $SU(N_c)$ invariants, so that group theoretical results can be used to decompose vectors into the bases. Multiplet bases, which decomposes the vector space into subspaces that transform under irreducible representations of $SU(N_c)$ fulfil these conditions. This type of bases have been used before for few external partons [12–17]. Recently a method of constructing the basis vectors for any number of external partons and any number of colours has been found [11].

Using curly lines for gluons will make many of the calculations very cluttered, so from now on gluons are denoted by plain lines without arrows. The completeness relation, eq. (23), can be used to find basis vectors that are $SU(N_c)$ invariants. The

method will be illustrated by an example amplitude with 6 external gluons

$$\begin{aligned}
 & \text{Diagram 1} = \sum_{\alpha_1} \frac{d_{\alpha_1}}{\text{Diagram 2}} \times \text{Diagram 3} = \\
 & = \sum_{\alpha_1, \alpha_2} \frac{d_{\alpha_1} d_{\alpha_2}}{\text{Diagram 4}} \times \text{Diagram 5} = \\
 & = \sum_{\alpha_1, \alpha_2, \alpha_3, \alpha_4} \frac{d_{\alpha_1} d_{\alpha_2} d_{\alpha_3} d_{\alpha_4}}{\text{Diagram 6}} \times \\
 & \quad \times \text{Diagram 7} = \\
 & = \sum_{\alpha_1, \alpha_2, \alpha_3} \frac{d_{\alpha_1} d_{\alpha_2} d_{\alpha_3}}{\text{Diagram 8}} \times \text{Diagram 9} \quad (48)
 \end{aligned}$$

where the first three steps are just applications of the completeness relation and the final step is from Schur's lemma, eq. (24). The choice of the 6 gluon basis vectors, here and in [11], are the colour structures

$$\begin{aligned}
 & \text{Diagram 10} \quad (49)
 \end{aligned}$$

The representation α_1 (α_2) must be in the tensor product $A \otimes A$ for the leftmost (rightmost) vertex to be non-zero. Similarly α_3 must be in the tensor product $A \otimes \alpha_1$ and $A \otimes \alpha_2$, for the remaining two vertices to be non-zero. The prefactor in eq. (48)

is then the weight that has to be evaluated. Taking the scalar product between two basis vectors of this form gives

(50)

Schur's lemma, eq. (24), ensures that the basis vectors are orthogonal if α_i is different from α'_i , for all i . But, as could be seen in eq. (18), there can be several instances of the same representation in a tensor product $((2,1)$ in the example). Hence if α_i is a different instance of the same representation as α'_i the basis vectors should be orthogonal, and is enforced in the construction of the basis vectors in [11].

This decomposition can be done for any number of external gluons in a similar manner. Completeness relations are used until all incoming gluons are in the same representation as all outgoing gluons, regardless of how many gluons there are on the incoming and outgoing sides. To note is that one can freely pick which gluons to put into a common representation, as long as it is done in the same way for all the colour structures, to enforce orthogonality. The basis vectors above do not contain any quarks, but they can also be dealt with using the same basis vectors with trivial changes. This is discussed in more detail in section 3.5.

The non-trivial step is to evaluate the weights for the basis vectors in eq. (48). It is only the vacuum bubble (a colour structure without external lines) that contains the grey blob that is complicated to evaluate. The dimensions are easy to calculate using eq. (10) and the two-vertex vacuum bubbles, known as Wigner $3j$ coefficients, are determined by the normalisation of the vertices. For the vacuum bubble with the grey blob one needs projection operators to ensure that the correct representations are in there.

2.3 Dynkin indices for arbitrary N_c

In multiplet bases tensor products between representations have to be decomposed, as was done in eq. (18). From the construction of the basis vectors in [11] there are only a very limited set of tensor products that must be considered. The only tensor products that are of interest are those between the adjoint representation of $SU(N_c)$, A , and any irreducible representation, $M \in A^{\otimes n_g}$. In this section an N_c -independent notation of representations and an N_c -independent decomposition of tensor products will be presented, starting from Young multiplication (see section 2.1.4).

This N_c -independent notation is similar to notation used in [18] to denote irreducible $SU(N_c)$ representations, it is a generalisation of Dynkin indices. The generalised notation consists of the first n Dynkin indices and the m last ones, leaving the possibility of any number of indices equal to zeros in between these two sets of indices. Choosing n and m determines how the representation is generalised to other N_c . If the

in $A \otimes q$, corresponding to placing the box of q in each of the rows of the Young diagram of A . Adding a box to row i of the Young diagram corresponding to M will increase α_i by 1, since it is now one box longer, and decrease α_{i-1} by 1, since its following row, row i , is now a box longer but row $i-1$ is unchanged. Hence all resulting representations from $A \otimes q$ can be written as

$$(\alpha_1, \dots, \alpha_{i-1} - 1, \alpha_i + 1, \dots, \alpha_{N_c-1}) \quad (54)$$

for $i = 1, \dots, N_c$, from placing the box in each row, if $(\alpha_1, \dots, \alpha_{N_c-1})$ are the indices for M . Note here that there are no Dynkin indices α_0 or α_{N_c} , the above notation is to be interpreted such that any change of those is to be disregarded. The reason to disregard changes to them is that there is not any row 0, and row N_c is always zero as columns of length N_c are removed for $SU(N_c)$ representations. Hence the decomposition of $M \otimes q$ can be written as

$$(\alpha_1, \dots, \alpha_{N_c-1}) \otimes q = \bigoplus_{i=1}^{N_c} (\alpha_1, \dots, \alpha_{i-1} - 1, \alpha_i + 1, \dots, \alpha_{N_c-1})|_{\alpha_{i-1} \geq 1}, \quad (55)$$

the $\alpha_i \geq 1$ enforces condition (i) of section 2.1.4. To note is that as mentioned after eq. (54) changes to α_0 are to be disregarded, so in eq. (55) the $i = 1$ representation is possible for any M . An example of eq. (55) for $SU(3)$ with $M = A = (1, 1)$ is

$$\begin{aligned} A \otimes q &= (2, 1) \oplus (0, 2) \oplus (1, 0), \\ 8 \otimes 3 &= 15 \oplus 6 \oplus 1. \end{aligned} \quad (56)$$

The conjugate of the fundamental representation is given by a Young diagram consisting of one column with $N_c - 1$ boxes (see the end of section 2.1.3 for conjugating representations)

$$\overline{\square} = \begin{array}{c} N_c - 1 \\ \square \\ \cdot \\ \cdot \\ \cdot \\ \cdot \\ \square \end{array}. \quad (57)$$

For $M' \otimes \bar{q}$ performing the procedure of section 2.1.4 for the $N_c - 1$ letters is simplified by condition (iv). As the boxes are added in order starting from a , only one box can be added to each row, otherwise the sequence is inadmissible. As there are $N_c - 1$ boxes, a box will be added to all but one row, referred to as row j from now on. In order to fulfil condition (iv), there is only one way of adding a box to every row except row j , so there will be N_c possible representations from this. An example of a possible and a disallowed representation in $M' \otimes \bar{q}$, is with $M' = (2, 1)$, two of the Young diagrams are then

$$\begin{array}{|c|c|c|c|} \hline & & & a \\ \hline & & & \\ \hline & & & \\ \hline b & & & \\ \hline \end{array}, \quad \begin{array}{|c|c|c|c|} \hline & & & b \\ \hline & & & \\ \hline & & & \\ \hline a & & & \\ \hline \end{array}. \quad (58)$$

Here the left Young diagram is allowed, a box has been added to each row except row 2 (this is an $SU(3)$ example, so there are only three rows) and the sequence ab is admissible. The right Young diagram would give the same representation, but is disallowed because ba is an inadmissible sequence. As the Dynkin indices are by definition the difference in number of boxes in two following rows the Dynkin indices do not change if a box is added to all rows. But there is one row where there is no box, so row j will be one box shorter than row $j + 1$ (where a box was added) and row $j - 1$ will be one longer than row j as row $j - 1$ also had a box added. Note the similarity to the case for $M \otimes q$, eq. (55), only a change of signs. Hence the decomposition of $M' \otimes \bar{q}$ can be written as

$$(\alpha'_1, \dots, \alpha'_{N_c-1}) \otimes \bar{q} = \bigoplus_{j=1}^{N_c} (\alpha'_1, \dots, \alpha_{j-1} + 1, \alpha_j - 1, \dots, \alpha'_{N_c-1}) \Big|_{\alpha_j \geq 1}. \quad (59)$$

The same applies to this equation as did to eq. (55), any change of α_0 and α_{N_c} is to be disregarded. The condition $\alpha_j \geq 1$ enforces condition (i) of section 2.1.4. Condition (ii) is trivially satisfied as there is only one of every letter, (iii) is satisfied since the boxes are by construction only added to rows 1 to N_c , and condition (iv) was applied when constructing eq. (59). In the above no, assumptions of M' need to be used, but the case of interest here is that $M' \in M \otimes q$. Applying this to the right hand side of the example, eq. (56), gives

$$\begin{aligned} \bar{q} \otimes [q \otimes (1, 1)] &= (1, 1) \oplus (3, 0) \oplus (2, 2) \oplus (1, 1) \oplus (0, 3) \oplus (0, 0) \oplus (1, 1) \\ \bar{3} \otimes [3 \otimes 8] &= 8 \oplus 10 \oplus 27 \oplus 8 \oplus \bar{10} \oplus 1 \oplus 8 \end{aligned} \quad (60)$$

Using eq. (55) and (59) the possible representations in $M \otimes (q \otimes \bar{q})$ can be seen as being of three different categories. First there is the representation that results from picking the $i = 1$ representation of eq. (55) and when multiplying that by \bar{q} picking the $j = 1$ representation. This will give the original representation M , and it is always possible, since condition (iii) is clearly satisfied if it is satisfied for M . The second category is picking any representation in eq. (55) except $i = 1$, and then picking the representation $j = i$ in eq. (59). For this category the result is again the original representation M , but here condition (iii) is no longer guaranteed to be fulfilled, because the representation picked from eq. (55) will contain $\alpha_{i-1} - 1$, which is negative if $\alpha_{i-1} = 0$. As i can take the values 2 to N_c there will be $N_c - 1$ representations of this type, one possible for every $\alpha_k \neq 0$ for $k = 1, \dots, N_c - 1$. The third category is all of the remaining representations, picking any i in eq. (55) and then picking $j \neq i$ in eq. (59).

The first category of the previous paragraph must be the representation coming from the singlet in $q \otimes \bar{q}$, since the other instances of the representation M come with an additional requirement on the Dynkin indices of M . From this the decomposition of $M \otimes A$, with $(\alpha_1, \dots, \alpha_{N_c-1})$ being the Dynkin indices of M , gives

- (a) For every $\alpha_i \neq 0$ there is one instance of M .

(b) All other representations can be enumerated by

$$\bigoplus_{i,j=1, i \neq j}^{N_c} (\alpha_1, \dots, \alpha_{i-1} - 1, \alpha_i + 1, \dots, \alpha_{j-1} + 1, \alpha_j - 1, \dots, \alpha_{N_c-1})|_{(\alpha_{i-1} \geq 1) \wedge (\tilde{\alpha}_j \geq 1)}, \quad (61)$$

note the tilde on $\tilde{\alpha}_j \geq 1$, it is there to indicate that it is not necessarily α_j . If $i - 1 = j$, then $\tilde{\alpha}_{j=i-1} = \alpha_{i-1} - 1$, so $\alpha_{i-1} \geq 2$ is required for the representation to be allowed.

The maximal number of possible representations in $M \otimes A$ is $N_c - 1$ from point (a) above and $N_c(N_c - 1)$ from point (b), giving $N_c^2 - 1$ in total, in agreement with [11]. Note that the requirement for all of these to be possible is that all of the Dynkin indices are ≥ 2 , so that a box can be added to any row and removed from the preceding row.

2.5 Generalisation to delimiter notation

The previous section showed that there can be at most $N_c^2 - 1$ representations in $M \otimes A$. If N_c goes to infinity, so does $N_c^2 - 1$, but the number of representations in the decomposition of $A^{\otimes n_g}$ does not. The change of Dynkin indices is always a decrease of an index and an increase of the following or preceding index, with the exceptions if $i, j = 1$ or N_c . If there are many zeros between the Dynkin indices on the left and on the right (how many will be shown later in this section), then adding an additional $\alpha_k = 0$ will not give rise to a new possible representation. It is preceded and succeeded by zeros, so i and j in (b) of section 2.4 cannot be chosen to be close to k . Hence, there are always a finite number of new multiplets if M is on the form of eq. (52).

There are two parts in showing that the delimiter notation of section 2.3 is possible to use along with the construction of the changes of the Dynkin indices of section 2.4. The first is to show that there are not any additional possible representations if $N_c \geq n + m + 2$. Secondly, as an arbitrary multiplet of $N_c^{min} = n + m$ or $N_c^{min+1} = n + m + 1$ can be expressed on the form of eq. (52), there should be $N_c(N_c - 1)$ possible representations different from M in $M \otimes A$ (only point 2 from the end of section 2.4) for those two N_c .

For M with a Young diagram given on the form

$$(\alpha_1, \alpha_2, \dots, \alpha_n, 0, \alpha_{N_c-m}, \alpha_{N_c-m+1}, \dots, \alpha_{N_c-1}) \quad (62)$$

or any higher N_c , i.e. there could be more consecutive zeros, it is easy to count the number of possible Young diagrams in $A \otimes M$. All possible ways of picking i of eq. (61) are $i = 1, \dots, n + 1$ and $i = N_c - m + 1, \dots, N_c$, since the other possibility would give -1 as the Dynkin index in the place where there is a zero in eq. (62). Similarly all the possible ways of picking j are $j = 1, \dots, n$ and $j = N_c - m, \dots, N_c$, for the same reason.

The maximal possible number of representations can be counted by looking at different choices of i and j . Starting with the possibilities when $i \neq n + 1$ and $j \neq N_c - m$, since then the requirement $i \neq j$ need to be taken into account. There are $n + m$ possibilities if $i \neq n + 1$, for each of them j can take $n + m - 1$ possible values (-1 from the requirement that $i \neq j$), giving $(n + m)(n + m - 1)$ possibilities. If $i = n + 1$,

j can take $n + m + 1$ values, and if $j = N_c - m$ then i can take $n + m + 1$ values, adding these two contributions and correcting for the double counting of $i = n + 1$, $j = N_c - m$, results in $2(n + m) + 1$ possibilities. That was an exhaustive list of all possibilities, so the total number is

$$N_{\max} = (n + m)(n + m - 1) + 2(n + m) + 1 = (n + m)(n + m + 1) + 1. \quad (63)$$

This number is valid for higher N_c than $n + m + 2$ (the number of Dynkin indices in eq. (62) plus 1) since additional zeros between α_n and $\alpha_{N_c - m}$ would not allow i or j to take any more values, since it would give a negative Dynkin index in place of one of the zeros.

The next step is to prove that constructing all of the N_{\max} representations and using the notational rule for which the lowest N_c for a Young diagram on the form of eq. (52) gives the correct number of possible Young diagrams for $N_c^{\min} = n + m$ and $N_c^{\min+1} = n + m + 1$. For $N_c^{\min} = n + m$ the representations resulting from either $i = n + 1$ or $j = N_c - m$ should be thrown away, since those are valid for $N_c \geq n + m + 1$ ($N_c \geq n + m + 2$ when $i = n + 1$ and $j = N_c - m$). This is the second contribution to N_{\max} in eq. (63), removing that gives

$$N_{\max} = (n + m)(n + m - 1) = N_c^{\min}(N_c^{\min} - 1).$$

For $N_c^{\min+1} = n + m + 1$ there is only one representation that is not allowed, when $i = n + 1$ and $j = N_c - m$, subtracting 1 from eq. (63) gives

$$N_{\max} = (n + m)(n + m + 1) = (N_c^{\min+1} - 1)N_c^{\min+1}.$$

So the generalised notation of section 2.3 can be used along with the rules at the end of section 2.4 without double counting any representations for $N_c = n + m$ or $N_c = n + m + 1$.

Now the rules for decomposing $A \otimes M$ for arbitrary N_c can be stated for the Young tableau with the indices

$$(\alpha_1, \alpha_2, \dots, \alpha_n | \alpha_{N_c - m}, \alpha_{N_c - m + 1}, \dots, \alpha_{N_c - 1}).$$

1. There is one instance of M for every $\alpha_k \neq 0$. Note that for $N_c = n + m$ there is only one M from α_n and $\alpha_{N_c - m}$, since they are only one Dynkin index and not two for that N_c (given that at least one of them is non-zero).
2. Construct all possible changes of Dynkin indices setting $\Delta\alpha_k = 0$ for $k = 1, \dots, N_c - 1$. Then go through $i = 1, \dots, n + 1$ and $i = N_c - m + 1, \dots, N_c$ and set

$$\Delta\alpha_{i-1} = -1$$

$$\Delta\alpha_i = 1.$$

For every value of i go through $j = 1, \dots, n$ and $j = N_c - m, \dots, N_c$ with the requirement that $i \neq j$, and add 1 to $\Delta\alpha_{j-1}$ and subtract 1 from $\Delta\alpha_j$. Note that there are no Dynkin indices with subscript 0 or N_c , so any manipulation of those two should be disregarded.

3. The possible multiplets $M' \subset A \otimes M$ are now the multiplets related to the Young tableaux resulting from changing the Dynkin indices of M according to all the possibilities of the preceding step.
4. Throw away any multiplet with negative Dynkin index.
5. The number of Dynkin indices in the resulting multiplets is equal to the N_c for which they are valid.

To clarify the last point: the resulting multiplets are valid for $N_c \geq n + m$ if there is not a 1 in either the $(n + 1)$ th or the $(N_c - m - 1)$ th places, if there is a 1 in either of the two then $N_c \geq n + m + 1$ and if there is a 1 in both $N_c \geq n + m + 2$. An example is

$$M' = (\alpha_1, \alpha_2, \dots, \alpha_n - 1, 1 | \alpha_{N_c - m}, \alpha_{N_c - m + 1}, \dots, \alpha_{N_c - 1} + 1)$$

here $i = n + 1$ and $j = N_c$ (i, j from section 2.4), this would be valid for $N_c \geq n + m + 1$. To note is that if M is a valid tableau for $N_c = n + m$, then the tableau in $A \otimes M$ with the highest lower limit of N_c has as limit $N_c \geq n + m + 2$ and there is only one such tableau.

2.6 Properties of the representations in $A^{\otimes n_g}$

From the previous section it is clear that the representations in $M \otimes A$ are highly constrained by the form of M . This can be used to find both the lowest n_g for which a representation occurs in $A^{\otimes n_g}$, as has been done in [11] where it was called first occurrence, and to enumerate all different representations in $A^{\otimes n_g}$.

2.6.1 First occurrence

To arrive at the first occurrence of a representation, M , it is useful to define two representations associated with M . First the quark diagram, Q , defined as

$$Q \equiv (\alpha_1, \dots, \alpha_n | 0, \dots, 0), \quad (64)$$

and second the antiquark diagram defined to be

$$\overline{Q'} \equiv \overline{(0, \dots, 0 | \alpha_{N_c - m}, \dots, \alpha_{N_c - 1})} = (\alpha_{N_c - 1}, \dots, \alpha_{N_c - m} | 0, \dots, 0). \quad (65)$$

The number of boxes in Q are given by

$$I = \sum_{k=1}^n k \alpha_k, \quad (66)$$

similarly for $\overline{Q'}$ the number of boxes is

$$J = \sum_{k=N_c - m}^{N_c - 1} (N_c - k) \alpha_k. \quad (67)$$

For the adjoint representation both Q and $\overline{Q'}$ are the fundamental representation, so $I = J = 1$.

Now it is of interest to see how I and J change when multiplying a representation, M , by A . There are four different cases of interest, the four different combinations of i and j of step 3 of section 2.5 being an index to the left or to the right of the delimiter $|$. The indices i and j can be on the left side (LS), $LS = \{1, \dots, n+1\}$ or on the right side (RS), $RS = \{N_c - m, \dots, N_c\}$. If $i \in LS$ then the quark diagram of M has one box added, so I increases by one, similarly if $j \in LS$ a box has been removed so that I decreases by one. This gives the result for the case when $i, j \in LS$, then I is unchanged, and so is of course J . If M has the Dynkin indices $(\alpha_1, \dots, \alpha_n | \alpha_{N_c-m}, \dots, \alpha_{N_c-1})$, adding a box for row $N_c - m$ or below, i.e. $i \in RS$, results in

$$\overline{Q'} \rightarrow \overline{(0, \dots, 0 | \alpha_{N_c-m}, \dots, \alpha_{i-1} - 1, \alpha_i + 1, \dots, \alpha_{N_c-1})} = (\alpha_{N_c-1}, \dots, \alpha_i + 1, \alpha_{i-1} - 1, \dots, \alpha_{N_c-m} | 0, \dots, 0). \quad (68)$$

The right-hand side of eq. (68) is an identical change as for $j \in LS$, a box is removed, so an $i \in RS$ results in one box less for the antiquark diagram, i.e. J decreases by one. If $j \in RS$ then

$$\overline{Q'} \rightarrow \overline{(0, \dots, 0 | \alpha_{N_c-m}, \dots, \alpha_{j-1} + 1, \alpha_j - 1, \dots, \alpha_{N_c-1})} = (\alpha_{N_c-1}, \dots, \alpha_j - 1, \alpha_{j-1} + 1, \dots, \alpha_{N_c-m} | 0, \dots, 0), \quad (69)$$

here a box is added to the antiquark diagram, hence J increases by one if $j \in RS$. Now the effect of all of the four cases can be stated

- $i, j \in LS$: I and J unchanged.
- $i, j \in RS$: I and J unchanged.
- $i \in LS$ and $j \in RS$: $I \rightarrow I + 1, J \rightarrow J + 1$
- $i \in RS$ and $j \in LS$: $I \rightarrow I - 1, J \rightarrow J - 1$

As was mentioned after equation (67) for the adjoint representation $I = J$, combined with the results above $I = J$ is true for all representations in $A^{\otimes n_g}$. It is also true that a representation with $I > n_g$ cannot be found in $A^{\otimes n_g}$, as multiplication with A can at most increase I by one, hence the highest possible I is n_g .

Before I can be proven to be the first occurrence of a representation it remains to show that all allowed quark diagrams can be formed by adding one box at a time. This would ensure that I does not just give the smallest n_g for which a representation can appear, but that it must appear for that n_g . It is clear that this is true as one way of creating any allowed Young diagram is by adding all boxes to row 1 first, one by one, then all boxes to row 2, etc. until row n . Hence the first occurrence of a representation $M \in A^{\otimes n_g}$ is given by

$$n_f(M) = \sum_{k=1}^n k \alpha_k = \sum_{k=N_c-m}^{N_c-1} (N_c - k) \alpha_k. \quad (70)$$

2.6.2 Representations in $A^{\otimes n_g}$

In this section the results of section 2.6.1 will be used to enumerate and count the number of different representations in $A^{\otimes n_g}$. For the counting of different representations

a possible concern here would be if some representations in the delimiter notation are different for a high enough N_c , but not for $N_c = n + m$. This could occur since the n th and the $(N_c - m)$ th Dynkin indices are added only for $N_c = n + m$. An example of this would be $(1|1)$ and $(2|0)$, for $N_c \geq 3$ they are different, but for $N_c = 2$ they are both (2) . Given the results of section 2.6.1 it is clear that $(2|0)$ is not present in $A^{\otimes n_g}$ for any n_g , as $I \neq J$ (eq. (66) and (67)). The cases where this is a problem is when α_n and α_{N_c-m} are redistributed, but there is only one way of distributing α_n and α_m without changing $\alpha_n + \alpha_m$ and having an equal number of boxes in Q and $\overline{Q'}$, i.e. $I = J$.

The unique representations in $A^{\otimes n_g}$ are the representations associated with all combinations of quark diagrams, Q , and antiquark diagrams, $\overline{Q'}$, with the same first occurrence and $n_f \leq n_g$. The number of unique representations is then the square of the number of possible Q diagrams for $n_f = 1, \dots, n_g$. The squaring is since any possible Q diagram is also a possible $\overline{Q'}$ diagram. A concern could be that representations in $A^{\otimes n_g-1}$ (or any other exponent lower than n_g) are not present any more in $A^{\otimes n_g}$, an example of this is that the singlet multiplied by a representation $M \neq 1$ does not contain the singlet. As was seen in point (a) of section 2.4 this is not a problem for any representation with at least one non-zero Dynkin index, hence it is only a potential issue for the singlet representation. This makes $A^{\otimes 1}$ a special case, since it does not contain the singlet, $A^{\otimes 2}$ contains a singlet, since $A \otimes A = (0|0) \oplus \dots$, the question now is if all $n_g \geq 2$ contain the singlet or not. The answer to this question is that they do, for all $n_g \geq 1$ there is at least one A , hence multiplying again by A will give at least one singlet representation, i.e. $A^{\otimes n_g-1}$ has at least one A , hence $A^{\otimes n_g}$ has at least one singlet, for $n_g \geq 2$.

All the unique representations can now be found for any n_g . As an example the unique representations for $n_g = 3$ are listed in table 1. For $n_f = 0$ there is only one possible Q (and hence $\overline{Q'}$) which is $Q = (0|0)$. For $n_f = 1$ there is again only one possibility $Q = (1|0)$. But for $n_f = 2$ there are more possibilities, then $Q = (2|0)$ and $Q = (0, 1|0)$ are possible. For $n_f = 3$ there are three possibilities: $Q = (3|0)$, $Q = (1, 1|0)$ and $Q = (0, 0, 1|0)$. All different representations in $A^{\otimes 3}$ are given in table 1. The sums in the multiplicity column are explicitly written out to indicate how many instances there are of that representation for different N_c , the first number is for the minimally allowed N_c , the second number is for one N_c higher, etc. So $3 + 5 + 1$ means that there are 3 A for $N_c = 2$, $3 + 5 = 8$ for $N_c = 3$ and 9 for $N_c = 4$. This can be compared to the result of [11]. There a different notation is used, denoting different representations by their column lengths, but the results here are in agreement with [11]. An example is $c3c21$, which means that the quark diagram (the numbers following the first c) consists of one column, 3 boxes long, and the antiquark (following the second c) is one column of length 2 and one of length 1. In the delimiter notation $c3c21$ is $(0, 0, 1|1, 1)$.

The number of different representations, Q , with a certain n_f is given by the number of allowed Young diagrams consisting of n_f boxes. From eq. (70) it can be seen that this is equivalent to the number of different ways of writing the integer n_f as a sum of integers. The function that gives this number for a given integer is called the partition

Table 1: Unique representations in $A^{\otimes 3}$.

n_f	$M \in A^{\otimes 3}$	$SU(3)$ dim	Min. N_c	Multiplicity
0	(0 0)	1	2	1+1=2
1	(1 1)	8	2	3+5+1=9
2	(2 2)	27	2	2+4=6
	(2 1,0)	10	3	4+2=6
	(0,1 2)	$\overline{10}$	3	4+2=6
	(0,1 1,0)	0	4	5+1=6
3	(3 3)	64	2	1
	(3 1,1)	35	3	2
	(1,1 3)	$\overline{35}$	3	2
	(3 1,0,0)	0	4	1
	(0,0,1 3)	0	4	1
	(1,1 1,1)	0	4	4
	(1,1 1,0,0)	0	5	2
	(0,0,1 1,1)	0	5	2
	(0,0,1 1,0,0)	0	6	1

function P , and is

$$P(n) = \sum_{i_n=0}^{\lfloor \frac{n}{3} \rfloor} \sum_{i_{n-1}=0}^{\lfloor \frac{n-i_n}{3} \rfloor} \dots \sum_{i_2=0}^{\lfloor \frac{n-i_n-i_{n-1}-\dots-i_3}{3} \rfloor} 1, \quad (71)$$

see appendix A for proof of this formula. The first few numbers of this function are

$$1, 2, 3, 5, 7, 11, 15, \dots \quad (72)$$

There is also an asymptotic solution for $P(n_f)$, first found in [21], which is

$$P(n_f) \propto \frac{1}{4n_f\sqrt{3}} e^{\pi\sqrt{2n_f/3}}. \quad (73)$$

As the number of unique Q with $n_f = k$ is given by $P(k)$, the number of unique representations in $A^{\otimes n_g}$ is given by

$$N_{\text{unique}}(n_g) = 1 + \sum_{k=1}^{n_g} P(k)^2, \quad \forall n_g \geq 2. \quad (74)$$

The added 1 in eq. (74) is from the singlet representation, which is also the reason for the limit of n_g . If $n_g = 1$, then there is just the adjoint representation, so $N_{\text{unique}}(1) = 1$. Note that eq. (74) counts the number of unique representations for $N_c \geq 2n_g$. This limit comes from (1|1) being valid for $N_c \geq 2$, and multiplying by A increases the

highest lower limit of N_c for which a representation is valid by 2. This is in agreement with the limit $N_c > n_f$ for the Q diagram, as the representations in $A^{\otimes n_g}$ are formed from Q and \bar{Q} , so if both have a limit of $N_c > n_f$, then the limit of the representation built from them is $N_c \geq n_f$ (equality as the n th and m th indices can be added), and the highest n_f is n_g .

For $N_c = 3$, only a small subset of the representations of eq. (74) are valid representations. The only quark diagrams that are of interest here are those with one or two Dynkin indices, as the quark diagrams with more Dynkin indices are not allowed for $N_c = 3$ ($n + m$ is larger than 3 for them). The number of such diagrams can be found by starting with the quark diagram $(n_f, 0|0)$, that is one possibility, then there is one possibility with $(n_f - 2, 1|0)$, and so on, the number of times 2 can be removed from n_f without getting a negative number is $\lfloor \frac{n_f}{2} \rfloor$, hence

$$P(n, 2) = 1 + \left\lfloor \frac{n_f}{2} \right\rfloor. \quad (75)$$

The number of possible representations for $N_c = 3$ with a given n_f is not just the square of this, since, for example, $(n_f - 2, 1|1, n_f - 2)$ is not allowed for $N_c = 3$. There is only one possible quark diagram with one Dynkin index, $(n_f|)$, this is the 1 in eq. (75). The number of representations with a given n_f is the number of possible combinations of quark and antiquark diagrams. This is $P(n, 2)$ squared, with the square of the second term of it removed as they are not valid representations for $N_c = 3$ (since $n + m = 4$), so

$$N_{\text{unique}}(n_f) = 1 + 2 \left\lfloor \frac{n_f}{2} \right\rfloor. \quad (76)$$

To get the total number of unique representations in $A^{\otimes n_g}$ for $SU(3)$ this has to be summed from 0 to n_g

$$N_{\text{unique}}(n_g) = \sum_{i=0}^{n_g} \left(1 + 2 \left\lfloor \frac{i}{2} \right\rfloor \right) = \left\lceil \frac{(n_g + 1)^2}{2} \right\rceil, \text{ for } n_g \geq 2. \quad (77)$$

For comparison, and to get a sense of the order of magnitude the result of eq. (74) and (77) have been calculated for the first number of gluons in table 2.

3 Feynman diagrams in multiplet bases

This section will start with introducing a known method for dealing with vacuum bubbles in group theoretical calculations, see for example [18]. This is then applied to a specific Feynman diagram for $3g \rightarrow 3g$. The method rewrites the weight, the bubble of eq. (48), in terms of smaller vacuum bubbles. Of interest is the number of small vacuum bubbles that are required to evaluate any leading order Feynman diagram for a given number of external gluons, this number is calculated in section 3.3.1.

3.1 Vacuum bubbles as sums over Wigner $3j$ and $6j$ coefficients

Rewriting a vacuum bubble into smaller vacuum bubbles only requires the application of completeness relations, eq. (23), and Schur's lemma, eq. (24). But it is useful

$$\begin{aligned}
&= \sum_{\alpha, \beta} \frac{d_\alpha \text{ (triangle)} d_\beta \text{ (triangle)}}{\ominus \ominus} \text{ (pentagon)} = \\
&= \sum_{\alpha, \beta, \gamma} \frac{d_\alpha \text{ (triangle)} d_\beta \text{ (triangle)}}{\ominus \ominus} \dots \text{ (hexagon)} = \\
&= \sum_{\alpha, \beta, \gamma, \delta} \frac{d_\alpha \text{ (triangle)} d_\beta \text{ (triangle)}}{\ominus \ominus} \dots \text{ (heptagon)} = \\
&= \sum_{\alpha, \beta, \gamma, \delta, \epsilon} \frac{d_\alpha \text{ (triangle)} d_\beta \text{ (triangle)}}{\ominus \ominus} \dots \text{ (octagon)} \dots \quad (79)
\end{aligned}$$

Two vertices are removed by using Schur's lemma, eq. (24), on the two vertex loop. This, in combination with the fact that the cross-channel relation, eq. (78), does not add any vertices to the bubble, results in two vertices having been removed. Hence this procedure can be applied to loops in the vacuum bubble until the vacuum bubble has been reduced to 4 vertices. The way to reduce the size of an arbitrarily large loop is to apply eq. (78) to any two adjacent legs, which results in a colour structure with a loop that is one vertex shorter (compare any two successive steps in eq. (79)).

Regardless of the number of edges in the loop, there are always two vertices removed. As there are more summations over new representations $(\alpha, \beta, \gamma, \dots)$ for larger loops, fewer terms have to be added if shorter loops are picked. This is expected, as the colour structure of two-vertex loops on propagators and vertex corrections are simple, but for larger loops it becomes more involved.

3.2 Example of decomposition

A typical example of the decomposition of a Feynman diagram for 6 external gluons is

$$= \sum_{\alpha_1, \alpha_2, \alpha_3} \frac{d_{\alpha_1} d_{\alpha_2} d_{\alpha_3}}{\text{diagrams}} \text{diagram} \quad (80)$$

where the equality is from applications of completeness relations and Schur's lemma, see eq. (48). The dimensions can easily be calculated from the Young tableaux of the representations, eq. (10), and since the vertices can be given any normalisation by specifying the Wigner $3j$ coefficients, only the vacuum bubble in the numerator is non-trivial. The smallest loop that can be found above is the vertex correction on the left side involving the α_1 representation. This is easily simplified by applying a completeness relation and Schur's lemma to cancel the summation

$$= \sum_{\psi} \frac{d_{\psi}}{\text{diagram}} \text{diagram} = \text{diagram} \quad (81)$$

In the basis vector, eq. (80), α_3 can have a first occurrence, n_f , up to 3. This comes from $\alpha_1 \in A \otimes A$ and $\alpha_3 \in \alpha_1 \otimes A$, and that the first occurrence can only increase by 1 per tensor product with A . The vertex correction of eq. (81) constraints it to $n_f \leq 2$. Using this for the weight in eq. (80) gives

$$= \frac{\text{diagram}}{\text{diagram}} \text{diagram} \quad (82)$$

All of the loops of the vacuum bubble are of length 4, which one to remove vertices from is immaterial. The loop chosen here is the outermost loop, containing α_1 and α_3 . Reducing it to Wigner $3j$ and $6j$ coefficients gives

$$\begin{aligned}
& \text{Diagram 1} = \sum_{\psi_1} \frac{d_{\psi_1}}{\text{Diagram 2}} \text{Diagram 3} = \\
& = \sum_{\psi_1, \psi_2, \psi_3} \frac{d_{\psi_1} d_{\psi_2} d_{\psi_3}}{\text{Diagram 4}} \text{Diagram 5} = \\
& = \sum_{\psi_1} d_{\psi_1} \frac{\text{Diagram 6} \text{Diagram 7}}{\left(\text{Diagram 8}\right)^2 \text{Diagram 9}} \text{Diagram 10}. \tag{83}
\end{aligned}$$

Using this, the weight has been completely reduced into Wigner $3j$ and $6j$ coefficients (it has 6 vertices in eq. (82) and every handled loop removes 2)

$$\begin{aligned}
& \text{Diagram 11} = \frac{\text{Diagram 12} \text{Diagram 13} \text{Diagram 14} \text{Diagram 15}}{\text{Diagram 16} \sum_{\psi_1} d_{\psi_1} \left(\text{Diagram 17}\right)^2 \text{Diagram 18}}. \tag{84}
\end{aligned}$$

Now the weight is expressed only in terms of vacuum bubbles with 2 or 4 vertices, and one new representation needs to be summed over. The procedure here does not require the representations in the basis vector to be specified until the right-hand side of eq. (84) has to be evaluated.

3.3 Representations and Wigner $6j$ coefficients

For the procedure stated in section 3.1 any loop can be chosen in the vacuum bubble. The projection operators are non-trivial to construct by the method in [11], so it is of interest that the representations that are introduced when removing loops do not have higher first occurrence than the first occurrences of the representations in the basis vectors. This section will show a possible way to choose the loops such that none of the Wigner $3j$ and $6j$ coefficients in the final expression contains representations with first occurrence larger than n_g , for a leading order Feynman diagram.

For this report only a subset of all possible vacuum bubbles have been considered, the ones that can occur in the decompositions of colour structures similar to eq. (48), and are on the form

(85)

The representations $\beta_1, \dots, \beta_n, \dots, \beta'_1$ are the representations of the basis vector and the blob of this equation only contains adjoint representations. Since all edges cannot be in arbitrary representations there is only a small subgroup of all possible vacuum bubbles that are to be evaluated. The idea behind this section is that the loop removal procedure of section 3.1, eq. (79), is to be applied carefully so that there will never be need of a vertex involving less than one adjoint representation. Applying the cross-channel relation, eq. (78), such that the introduced representation α has first occurrence larger than n_g would require the projectors for those representations to be constructed. This is not desirable because it is time-consuming to construct the projectors by the method of [11].

It suffices to check that the first occurrence will not be a problem for the basis vectors with the highest first occurrence, hence it is assumed that β_i and β'_i , in eq. (85), have first occurrence $i + 1$ in the following. The representation β_1 , is composed of two gluons, hence its highest first occurrence is 2. For β_2 one additional gluon is added, so first occurrence can be at most 3. Hence in the rest of the section it will be assumed that $n_f(\beta_i) = n_f(\beta'_i) = i + 1$. In the following it is useful to differentiate between the adjoint representations in the blob of eq. (85), since they are present for any basis vector, and the representations β_i, β'_i and any additional representations coming from the cross-channel relation. Hence any mention of gluons or the adjoint representation in this section refer exclusively to plain edges and arbitrary representations refer only to the double edges. In the following, possible choices of loops are first given, then the application of the cross-channel relation, eq. (78), on them is examined, to show that too high first occurrence of representations is not an issue for the presented loops.

A loop from eq. (85) can be found by checking if any vertex in the blob has two edges connected to the chain of basis vector representations. At tree level such a loop can always be found. Since there are no loops in the colour structure, there must be at least two vertices that are only connected by one edge to the rest of the colour structure. A loop found like this will be of the form

$$(86)$$

Another type of loop can occur after enough vertices have been removed is

$$(87)$$

There is yet another type of loop which will not increase n_f past n_g , but will require a small number of extra Wigner coefficients (this is discussed in more detail in section 3.6),

$$(88)$$

The important aspect of their forms is the number of triple-gluon vertices from the blob in them. Any of the arbitrary representations can be swapped for gluon edge, given that the number of triple-gluon vertices from the blob does not increase. It is sufficient to only contract loops on the forms of eq. (86) and (87). The need for the second type of loop is because for large enough vacuum bubbles all of the triple-gluon vertices from the blob might have been removed, leaving only loops like eq. (87). It is not always possible to find loops on the form of (88), but they are included as at some step they can be possible, and be shorter than picking a loop on the form of (86). The trade-off with them is the need of more Wigner $6j$ coefficients, but only ones that do not require representations with higher n_f than n_g .

When applying the cross-channel relation μ or ν should be a gluon, and so should either ρ and σ , to ensure that each vertex has at least one gluon. One way to apply the cross-channel relation, eq. (78), is to apply it to one of the legs in arbitrary representations of the loop, β_i (or β_n) in all the example loops. The cross-channel

Table 3: Highest first occurrences for ψ in eq. (90).

	n_f			n_f		n_f	
β_{j-1}	n	$n-1$	$n-2$	n	$n-1$	n	n
β_j	$n-1$	n	$n-1$	n	n	$n-1$	n
β_{j+1}	$n-2$	$n-1$	n	$n-1$	n	n	n
ψ	$n-1$	n	$n-1$	n	n	$n+1$	$n+1$

relation is then applied to something on the form of

$$(89)$$

where the dots represent that the loop can be of any size. If μ is taken to be β_{j-1} and ν the gluon pointing downwards and to the left, then the resulting colour structure is

$$\sum_{\psi} \frac{d_{\psi}}{\text{triangle and circles}} \beta_{j-1} \text{ chain diagram } \beta_{j+1} \beta_{j+2} . \quad (90)$$

Since the representation ψ is in the tensor product $\beta_{j-1} \otimes A$ and $\beta_{j+1} \otimes A$ its first occurrence can at most be $n_f(\psi) \leq \max(\beta_{j-1}, \beta_{j+1}) + 1$ (see section 2.6.1). Table 3 enumerates all possible first occurrences of β_{j-1} , β_j and β_{j+1} , and the corresponding highest first occurrences for ψ . In the table n is the highest first occurrence of the three representations that are involved in the cross-channel relation, i.e. $n = \max(n_f(\beta_{j-1}), n_f(\beta_j), n_f(\beta_{j+1}))$. Only the highest possible first occurrence is shown in the above table, for example for the second column of possible first occurrences the first occurrence of ψ could also be $n-1$ or $n-2$. To note in the table is that the first occurrence of ψ cannot exceed n unless there are two representations with first occurrence n separated by one representation with first occurrence $n-1$ or n . Here it is not of interest if $n < n_g$, since then it is not a problem increasing the first occurrence. If $n = n_g$ then the two last columns are problematic, but for the basis vectors for $2n_g$ external gluons only the first three columns can occur and for $2n_g + 1$ external gluons the two columns following those can occur as well.

In the initial vacuum bubble, eq. (85), the double line representations of the basis vectors are in a chain. If the cross-channel is applied as specified in the previous paragraph then the loop will contain a segment of this chain. After the loop has been dealt

3.3.1 Wigner $3j$ and $6j$ coefficients

The Wigner $3j$ coefficients account for the normalisation of the vertices. As the normalisation is arbitrary, one can for example set all of the normalisations such that the $3j$ coefficients are all one or zero. This can be done for all coefficients of the form

$$\begin{array}{c} \text{---} \\ \text{---} \\ \text{---} \end{array} \begin{array}{c} \alpha \\ \beta \end{array} \quad (93)$$

Different instances of vertices connecting the same representations are orthogonal by construction, such that eq. (93) for different instances of α - β -gluon vertices are zero. As was seen in the end of section 2.4, this only occurs for $\alpha = \beta$. Since the completeness relation, eq. (23), should be a decomposition into different subspaces. It is always possible, as will be illustrated, to choose the vertices such that interchange of two legs is symmetric or antisymmetric, i.e. the interchange of two legs only gives a factor of ± 1 .

In the following Yutsis' notation to denote vertex ordering will be used [22],

$$\begin{array}{c} \alpha \\ \text{---} \\ \text{---} \\ \beta \end{array} \begin{array}{c} \gamma \\ \text{---} \\ \text{---} \end{array} = \begin{array}{c} \alpha \\ \text{---} \\ \text{---} \\ \beta \end{array} \begin{array}{c} \gamma \\ \text{---} \\ \text{---} \end{array} \quad (94)$$

For the vertices with one adjoint representation and two arbitrary representations, $\alpha \neq \beta$, one can use a completeness relation to get

$$\begin{array}{c} \alpha \\ \text{---} \\ \text{---} \\ \beta \end{array} = \sum_{\psi} \frac{d_{\psi}}{\begin{array}{c} \psi \\ \text{---} \\ \text{---} \\ \beta \end{array}} \begin{array}{c} \alpha \\ \text{---} \\ \text{---} \\ \beta \end{array} \begin{array}{c} \psi \\ \text{---} \\ \text{---} \end{array} = \frac{\begin{array}{c} \alpha \\ \text{---} \\ \text{---} \\ \beta \end{array}}{\begin{array}{c} \alpha \\ \text{---} \\ \text{---} \\ \beta \end{array}} \begin{array}{c} \alpha \\ \text{---} \\ \text{---} \\ \beta \end{array} \quad (95)$$

The reason for requiring $\alpha \neq \beta$ is that there is only one vertex connecting α , β and ψ . Changing the order twice should bring back the original vertex, hence the constant in eq. (95) must be ± 1 .

For the vertices with $\alpha = \beta$ the summation in eq. (95) is only partly cancelled, it will still run over all different vertices connecting α , α and A . Changing eq. (95) to account for this, dropping the representation labels, and introducing the labels i and j , to denote the intended vertex (for example $j = f, d$ for the three-gluon vertices), gives

$$\begin{array}{c} i \\ \text{---} \\ \text{---} \\ \text{---} \end{array} = \sum_j \frac{\begin{array}{c} j \\ \text{---} \\ \text{---} \\ j \end{array}}{\begin{array}{c} j \\ \text{---} \\ \text{---} \\ j \end{array}} \begin{array}{c} j \\ \text{---} \\ \text{---} \\ \text{---} \end{array} = \sum_j C_{ij} \begin{array}{c} j \\ \text{---} \\ \text{---} \\ \text{---} \end{array} \quad (96)$$

The normalisation of the vertices is set such that

$$\begin{array}{c} i \\ \circlearrowleft \\ \circlearrowright \\ i \end{array} = \begin{array}{c} j \\ \circlearrowleft \\ \circlearrowright \\ j \end{array}, \quad \forall i, j \quad (97)$$

and

$$\begin{array}{c} i \\ \circlearrowleft \\ \circlearrowright \\ i \end{array} = \begin{array}{c} i \\ \circlearrowright \\ \circlearrowleft \\ i \end{array}, \quad \forall i. \quad (98)$$

If normalisation conditions above are used, another equality that will be of use is

$$\begin{aligned} \begin{array}{c} i \\ \diagup \\ \diagdown \\ \text{---} \end{array} &= \sum_j \frac{\begin{array}{c} i \\ \circlearrowleft \\ \circlearrowright \\ j \end{array}}{\begin{array}{c} j \\ \circlearrowleft \\ \circlearrowright \\ j \end{array}} \begin{array}{c} j \\ \diagup \\ \diagdown \\ \text{---} \end{array} = \sum_j \frac{\begin{array}{c} i \\ \circlearrowright \\ \circlearrowleft \\ j \end{array}}{\begin{array}{c} j \\ \circlearrowleft \\ \circlearrowright \\ j \end{array}} \begin{array}{c} j \\ \diagup \\ \diagdown \\ \text{---} \end{array} = \\ &= \sum_j \frac{\begin{array}{c} j \\ \circlearrowleft \\ \circlearrowright \\ i \end{array}}{\begin{array}{c} i \\ \circlearrowleft \\ \circlearrowright \\ i \end{array}} \begin{array}{c} j \\ \diagup \\ \diagdown \\ \text{---} \end{array} = \sum_j C_{ji} \begin{array}{c} j \\ \diagup \\ \diagdown \\ \text{---} \end{array} = \\ &= \sum_j (C^T)_{ij} \begin{array}{c} j \\ \diagup \\ \diagdown \\ \text{---} \end{array}. \quad (99) \end{aligned}$$

The second step is just connecting the gluon above the other two edges, instead of under it (does not change anything since the orders of the vertices are unchanged). In the third step eq. (97) and then eq. (98) are used for the denominator. For the numerator the two vertices are just displaced.

Writing the normal ordered vertex as a vertex that has had its order changed twice and using eq. (96) and eq. (99) gives

$$\begin{aligned} \begin{array}{c} i \\ \diagup \\ \diagdown \\ \text{---} \end{array} &= \begin{array}{c} i \\ \diagup \\ \text{---} \\ \diagdown \\ i \end{array} = \sum_j C_{ij} \begin{array}{c} j \\ \diagup \\ \text{---} \\ \diagdown \\ j \end{array} = \\ &= \sum_j C_{ij} \begin{array}{c} j \\ \diagup \\ \diagdown \\ \text{---} \end{array} = \sum_{j,k} C_{ij} (C^T)_{jk} \begin{array}{c} k \\ \diagup \\ \diagdown \\ \text{---} \end{array}. \quad (100) \end{aligned}$$

In order for the left-hand side to be equal to the right-hand side of eq. (100) the constants C_{ij} have to fulfil $\sum_j C_{ij}(C^T)_{jk} = \delta_{ik}$. The matrix C with components C_{ij} is then an orthogonal matrix, i.e. $C^{-1} = C^T$. The eigenvectors of an orthogonal matrix can be chosen to be orthogonal. Another property of C can be shown similarly,

$$\begin{aligned}
 & \text{Diagram with two incoming lines from the left and one outgoing line to the top-right, labeled } i \\
 & = \sum_j C_{ij} \text{Diagram with two incoming lines from the left and one outgoing line to the top-right, labeled } j \\
 & = \sum_{j,k} C_{ij} C_{jk} \text{Diagram with two incoming lines from the left and one outgoing line to the top-right, labeled } k
 \end{aligned} \tag{101}$$

In order for this to hold the constants C_{ij} have to fulfil $\sum_j C_{ij} C_{jk} = \delta_{ik}$, a matrix for which $C = C^{-1}$ is called an involutory matrix. A matrix that is involutory can be diagonalised with all eigenvalues being ± 1 [23]. Hence new vertices can be chosen, that are linear combinations of the vertices i , with eigenvalues ± 1 under the change of ordering of the edges.

Since the matrix C is orthogonal and involutory it can be diagonalised with eigenvalues ± 1 , i.e. it is either symmetric under interchange of legs or it is antisymmetric, and the eigenvectors can be chosen to be orthogonal. This means that the condition

$$\text{Diagram with two incoming lines from the left and one outgoing line to the top-right, labeled } i \text{ and } j \text{ with } \alpha \text{ and } -\alpha \text{ on the legs} = B^\alpha \delta_{ij}, \tag{102}$$

still holds, the vertices are still orthogonal after redefining them as vertices that have a specific symmetry under changing of order of the legs.

3.4 Required Wigner $6j$ coefficients and their symmetries

The only possible Wigner $6j$ coefficients that can occur with the requirement that at least one edge connected to every vertex is a gluon are

$$\text{Diagram of a triangle with three vertices and three edges, labeled } \alpha, \beta, \gamma \tag{103}$$

and

$$(104)$$

How many of these coefficients are there then? They can be counted by constructing every unique representation valid for a given number of gluons, as is done in section 2.6.2, then checking how many vertices there are that can be connected three (for eq. (103)) or four times (for eq. (104)) in a row giving the original representation. For QCD an overestimate is given by taking the number of unique representations in $A^{\otimes n_g}$, given by eq. (77), and multiplying it by $N_c^2 - 1$ to the power of the number of vertices, with $N_c = 3$. Since from section 2.4 there are at most $N_c^2 - 1$ representations in $A \otimes M$. Hence an upper limit for the number of required coefficients is

$$N_{\text{Wigner coefficients}}(n_g) \leq (8^3 + 8^4) \left[\frac{(n_g + 1)^2}{2} \right]. \quad (105)$$

The interesting part here is the scaling, and not the exact numbers. The total number of required coefficients scales quadratically in the number of external gluons.

For the symmetry relations to have a simpler form it is useful to define the vertices such that the conjugate of a vertex is related to the vertex for the conjugate of the representations. If $\alpha \neq \beta$, then the normalisation and colour structures should be chosen such that

$$\left(\begin{array}{c} \alpha \quad \beta \\ \text{---} \text{---} \\ \text{---} \\ \text{---} \end{array} \right)^* = \begin{array}{c} \bar{\alpha} \quad \bar{\beta} \\ \text{---} \text{---} \\ \text{---} \\ \text{---} \end{array}, \quad (106)$$

for $\alpha = \beta$ they are instead defined as

$$\left(\begin{array}{c} \alpha \quad i \quad \alpha \\ \text{---} \text{---} \\ \text{---} \\ \text{---} \end{array} \right)^* = \sigma(\alpha, i) \begin{array}{c} \bar{\alpha} \quad i \quad \bar{\alpha} \\ \text{---} \text{---} \\ \text{---} \\ \text{---} \end{array}, \quad (107)$$

where $\sigma(\alpha, i)$ is 1 if the vertex i is symmetric under change of leg ordering and -1 if it is antisymmetric. The reason for the additional minus sign for the antisymmetric vertices between the same representation is for similarity to the triple-gluon vertex, eq. (31), which gets a minus sign under conjugation.

The coefficients have many symmetries, greatly reducing the number of independent coefficients. One obvious symmetry of the coefficient of eq. (103) is cyclic permutations of α, β, γ , i.e.

$\begin{array}{c} \alpha \quad \gamma \\ \downarrow \quad \uparrow \\ \text{---} \beta \text{---} \\ \uparrow \quad \downarrow \end{array} = \begin{array}{c} \gamma \quad \beta \\ \downarrow \quad \uparrow \\ \text{---} \alpha \text{---} \\ \uparrow \quad \downarrow \end{array} . \quad (108)$

The coefficient of eq. (104) also has a cyclic permutation symmetry, but with all 4 representations. But with the difference that all 4 vertices have to be inverted. This is easily seen by drawing it as a square, rotating it and then drawing it in the original shape

$\begin{array}{c} \delta \\ \downarrow \quad \uparrow \\ \alpha \quad \gamma \\ \downarrow \quad \uparrow \\ \text{---} \beta \text{---} \\ \uparrow \quad \downarrow \end{array} = \begin{array}{c} \delta \\ \leftarrow \quad \rightarrow \\ \alpha \quad \gamma \\ \downarrow \quad \uparrow \\ \text{---} \beta \text{---} \\ \leftarrow \quad \rightarrow \end{array} = \\ = \begin{array}{c} \gamma \\ \leftarrow \quad \rightarrow \\ \delta \quad \beta \\ \downarrow \quad \uparrow \\ \text{---} \alpha \text{---} \\ \leftarrow \quad \rightarrow \end{array} = \begin{array}{c} \gamma \\ \downarrow \quad \uparrow \\ \delta \quad \beta \\ \downarrow \quad \uparrow \\ \text{---} \alpha \text{---} \\ \uparrow \quad \downarrow \end{array} . \quad (109)$

As the Wigner coefficients are composed of quark lines and symmetrizers and anti-symmetrizers of these, they are polynomials in N_c . The expansion of the symmetrizers and antisymmetrizers result in a number of closed quark loops, which each equal a factor of N_c . Hence they are real numbers, invariant under complex conjugation. The effect of complex conjugation on birdtracks is reversing the the arrows on all of the lines. Care has to be taken, as there can be lines inside a vertex, as for the triple-gluon vertex eq. (31), which can give a sign change in reversing the order of lines in the vertex. This gives the symmetry relation

$\begin{array}{c} \alpha \quad \gamma \\ \downarrow \quad \uparrow \\ \text{---} \beta \text{---} \\ \uparrow \quad \downarrow \end{array} = (-1)^i \begin{array}{c} \bar{\alpha} \quad \bar{\gamma} \\ \downarrow \quad \uparrow \\ \text{---} \bar{\beta} \text{---} \\ \uparrow \quad \downarrow \end{array} . \quad (110)$

and

$$\begin{array}{c} \alpha \\ \delta \\ \gamma \\ \beta \end{array} = (-1)^i \begin{array}{c} \bar{\alpha} \\ \bar{\delta} \\ \bar{\gamma} \\ \bar{\beta} \end{array} , \quad (111)$$

where i is the number of vertices between the same representation that are antisymmetric under the change of ordering of the legs (see eq. (107)).

Another symmetry can be found by switching the places of the lower left and lower right vertices of eq. (103) and (104). This will change the order of every vertex of the coefficient, giving symmetry factors, but relating it to the coefficients with the representations going in the opposite direction

$$\begin{array}{c} \alpha \\ \gamma \\ \beta \end{array} = \begin{array}{c} \gamma \\ \alpha \\ \beta \end{array} = \begin{array}{c} \bar{\gamma} \\ \bar{\alpha} \\ \bar{\beta} \end{array} . \quad (112)$$

For the coefficients on the form of eq. (104) this is

$$\begin{array}{c} \alpha \\ \delta \\ \gamma \\ \beta \end{array} = \begin{array}{c} \gamma \\ \delta \\ \alpha \end{array} = \begin{array}{c} \beta \\ \gamma \\ \delta \end{array} . \quad (113)$$

3.4.1 Counting the required Wigner coefficients

If only loops on the forms of eq. (86) and (87) are chosen the Wigner coefficients do not need to have vertices connecting two $n_f = n_g$ representations, for $2n_g$ external gluons. This can be seen for the coefficients on the form of eq. (104) by looking at table 3 in section 3.3. For the first three columns which are the only ones that can occur for $N_g = 2n_g$ only column three has two representations with the highest first occurrence. But as ψ connects to β_{j-1} and β_{j+1} , and not to β_j there is no vertex connecting the two representations with a first occurrence that could be n_g .

The coefficients on the form of eq. (103) occur in the final steps of handling the loops, see eq. (91) and (92). Only one of the representations of eq. (91) can have $n_f = n_g$, as that is the case in the initial basis vector and section 3.3 showed that

Table 4: Required number of Wigner coefficients for N_g external gluons.

N_g	4	6	8	10	12
$N_c \geq N_g$	52	396	2 126	9 059	32 702
$N_c = 3$	38	130	277	479	736

handling the loops does not change that fact. For eq. (92) the highest possible first occurrence of ψ is when $n_f(\alpha) = n_f(\gamma) = n_g - 1$ and $n_f(\beta) = n_g$, then $n_f(\psi)$ can be n_g . Hence if such loops are taken coefficients on the form of eq. (103) with two representations with $n_f = n_g$ are required as well. There is no need for such coefficients with three $n_f = n_g$ representations though, since the coefficients from eq. (92) would contain either α or β , which had $n_f = n_g - 1$.

From the above, the representations in the Wigner coefficients are constrained. In the coefficients on the form of eq. (104) two representations connected at a vertex cannot both have $n_f = n_g$. For eq. (103) two representations can have $n_f = n_g$, if loops like eq. (88) are picked, but all three representations cannot have first occurrence $n_f = n_g$. Using this and the symmetries of eq. (108), (109), (112) and (113), one can count the required number of coefficients, these numbers are stated in table 4.

3.5 External Quarks

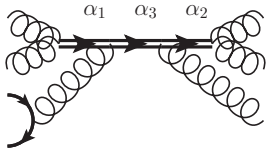
So far only gluons have been considered, but it is also possible to deal with quarks in a similar manner. The Feynman rules for QCD only connect one gluon to a quark and an antiquark, meaning that the number of external quarks must be equal to the number of external antiquarks (if all quarks are considered outgoing or ingoing). This means that the quarks and antiquarks can always be considered as quark-antiquark pairs. The completeness relation, eq. (23), can be applied to every pair, as in eq. (43), which gives

$$q \otimes \bar{q} = 1 \oplus A. \quad (114)$$

The basis vectors can be chosen to be (curly lines are used for gluons here)


(115)

and


(116)

If there are more quark-antiquark pairs then all combinations of them being in the singlet or adjoint representation give different basis vectors (e.g. for two pairs one can be in the singlet representation and the other in the adjoint representation).

The method of removing vertices from loops can be applied in the same manner even with quarks. Inside the weights, coming from usage of Schur's lemma after application of all completeness relations, as in eq. (48), there will be closed quark loops. The method in [11] is for projectors where the quarks and antiquarks have been paired up, so it is a general construction of projectors for $A^{\otimes n_g}$, and not for $q \otimes M$. For this reason the quark loops should be rewritten in terms of the adjoint representation first, and then the method of decomposition is unchanged from the case with only gluons. If there are quark loops inside the bubble of eq. (85), then the loops that are picked (eq. (86), (88) and (87)) might contain quark edges. Using the cross-channel relation could then result in the summed over representation, α , being in the tensor product $q \otimes M$, which would then require projectors for such tensor products. This can be avoided by applying completeness relations on the quarks in a loop

$$(117)$$

In both terms the rest of the loop, shown by the dots, has become 1 or 2 vertices shorter. The vertex correction of the second term can be rewritten in terms of only triple-gluon vertices by usage of the symmetric triple-gluon vertex

$$(118)$$

Using this and eq. (31) quark loops with three gluons attached can be expressed in terms of triple-gluon vertices, for example

$$(119)$$

This is similar to the procedure for the trace bases (see section 2.2.2), but now quark loops are removed in favour of triple-gluon vertices. Another type of Wigner $6j$ coefficients will be required, the same form as eq. (103) but with a symmetric triple-gluon

vertex. The number of additional Wigner coefficients that are required is small, since there are fewer of eq. (103) than of eq. (104) so the numbers of section 3.4.1 are very close, especially for many external gluons.

3.6 Evaluation of Wigner coefficients

Using the basis vectors of [11] (see appendix B for notes on the sign of some of the vectors) all the required Wigner coefficients for 6 external gluons have been calculated in the ColorMath program [24]. The calculated coefficients are sufficient if no loop of the form of eq. (88) have been picked. If such loops are also picked then additional Wigner coefficients are required, as stated in section 3.4.1.

For the evaluation of the Wigner coefficients some normalisation of the vertices must be picked, or left as a free parameter, like T_R of eq. (30). In the basis vectors a specific normalisation has been picked, since the scalar product of any basis vector with itself is normalised to 1. The scalar product of a vector with itself, from eq. (35), can be reduced to factors of Wigner $3j$ coefficients and representation dimensions by the usage of Schur's lemma,

$$\begin{aligned}
 & \text{Diagram 1} = \text{Diagram 2} \\
 & = \frac{\text{Diagram 3}}{d_{\alpha_1}} \frac{\text{Diagram 4}}{d_{\alpha'_1}} \times \\
 & \times \text{Diagram 5} = \text{Diagram 6} \\
 & = \left(\frac{\text{Diagram 7}}{d_{\alpha_1}} \frac{\text{Diagram 8}}{d_{\alpha_2}} \dots \frac{\text{Diagram 9}}{d_{\alpha_n}} \right) \left(\frac{\text{Diagram 10}}{d_{\alpha'_1}} \frac{\text{Diagram 11}}{d_{\alpha'_2}} \dots \frac{\text{Diagram 12}}{d_{\alpha'_n}} \right) \text{Diagram 13} .
 \end{aligned} \tag{120}$$

The last loop just gives the dimension of the representation α_n . The basis vectors are normalised such that eq. (120) is 1. In the calculation of the Wigner $6j$ coefficients for

6 external gluons the normalisation was instead chosen such that the factor of all of the Wigner $3j$ coefficients were 1. To change to this normalisation the vectors of [11] were multiplied by

$$\frac{1}{\sqrt{d_{\alpha_1} \dots d_{\alpha_{n-1}} d_{\alpha_n} d_{\alpha'_m} \dots d_{\alpha'_1}}}. \quad (121)$$

The Wigner $6j$ coefficients on the form of eq. (104) can be evaluated from the scalar products of basis vectors according to

$$\text{Tr} \left[\begin{array}{c} \alpha_1 \quad \alpha_n \quad \alpha'_n \quad \alpha'_1 \\ \vdots \quad \vdots \quad \vdots \quad \vdots \\ \alpha_{n-1} \quad \alpha'_{n-1} \quad \alpha'_{n-1} \quad \alpha_{n-1} \\ \vdots \quad \vdots \quad \vdots \quad \vdots \end{array} \right]. \quad (122)$$

As in eq. (120) this will give factors of Wigner $3j$ coefficients. But using the renormalised basis vectors the Wigner $3j$ coefficients are 1, so every application of Schur's lemma gives a factor of one over the dimension of a representation. Hence eq. (122) is equal to

$$\begin{aligned} & \frac{1}{d_{\alpha_1} \dots d_{\alpha_{n-1}} d_{\alpha'_1} \dots d_{\alpha'_n-1}} \begin{array}{c} \alpha_{n-1} \\ \alpha_n \quad \alpha'_n \\ \alpha'_{n-1} \end{array} = \\ & = \frac{1}{d_{\alpha_1} \dots d_{\alpha_{n-1}} d_{\alpha'_1} \dots d_{\alpha'_n-1}} \begin{array}{c} \alpha_{n-1} \\ \alpha_n \quad \alpha'_n \\ \alpha'_{n-1} \end{array} = \\ & = \frac{1}{d_{\alpha_1} \dots d_{\alpha_{n-1}} d_{\alpha'_1} \dots d_{\alpha'_n-1}} \begin{array}{c} \alpha'_{n-1} \\ \alpha'_n \quad \alpha_n \\ \alpha_{n-1} \end{array}. \quad (123) \end{aligned}$$

For the Wigner $6j$ coefficients on the form of eq. (103) with only one representation having $n_f = n_g$ the 5 and 6 gluon basis vectors are sufficient. If the coefficients with two or more representations with $n_f = n_g$ are needed (i.e. if loops like eq. (88) are handled) then vertices between such representations must be constructed. Instead of 5 gluon basis vectors, 7 gluon basis vectors would be required, in [11] it is described how to construct the basis vectors for $2n_g + 1$ external gluons with the projectors for $2n_g$ projectors. The 5 gluon basis vector is contracted with the 6 gluon basis vector as follows

$$\begin{aligned}
 & \text{Tr} \left[\begin{array}{c} \alpha_1 \quad \alpha_{n-1} \alpha'_{n-1} \quad \alpha'_1 \quad \alpha'_1 \quad \alpha'_{n-1} \alpha_n \quad \alpha_{n-1} \quad \alpha_1 \\ \text{---} \text{---} \text{---} \text{---} \text{---} \text{---} \text{---} \text{---} \\ \text{---} \text{---} \text{---} \text{---} \text{---} \text{---} \text{---} \text{---} \\ \text{---} \text{---} \text{---} \text{---} \text{---} \text{---} \text{---} \text{---} \\ \text{---} \text{---} \text{---} \text{---} \text{---} \text{---} \text{---} \text{---} \end{array} \right] = \\
 & \frac{1}{d_{\alpha_1} \dots d_{\alpha_{n-1}} d_{\alpha'_1} \dots d_{\alpha'_{n-1}}} = \begin{array}{c} \alpha_{n-1} \\ \text{---} \text{---} \text{---} \text{---} \\ \alpha'_{n-1} \quad \alpha_n \\ \text{---} \text{---} \text{---} \text{---} \\ \alpha_{n-1} \end{array} = \\
 & = \frac{1}{d_{\alpha_1} \dots d_{\alpha_{n-1}} d_{\alpha'_1} \dots d_{\alpha'_{n-1}}} \begin{array}{c} \alpha_{n+1} \\ \text{---} \text{---} \text{---} \text{---} \\ \alpha_n \\ \text{---} \text{---} \text{---} \text{---} \\ \alpha_{n-1} \end{array} . \quad (124)
 \end{aligned}$$

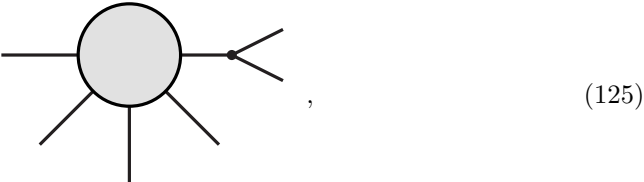
Where the first step is from applying Schur's lemma and using that the Wigner $3j$ coefficients are all normalised to 1.

For 6 external gluons the coefficients from eq. (123) and (124) have been calculated and can be found in appendix C.

4 Recursion relation colour structures in multiplet bases

This section will deal with multiplet basis vectors radiating gluons from one of their legs. Such colour structures can be of interest in recursion relations for amplitudes and for parton showers. The recursion relations relate the amplitudes for a process with N_g external gluons to one with $N_g - 1$ external gluons. This is very interesting as it is

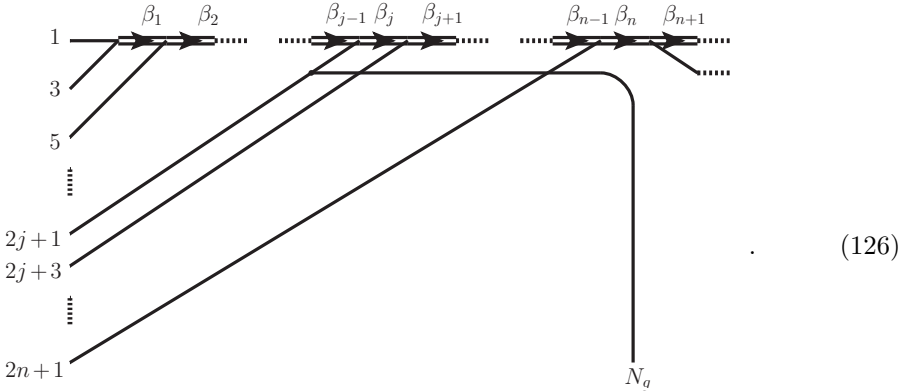
a way of getting around the $\sim N_g!$ scaling of the number of Feynman diagrams. The colour structures are on the form



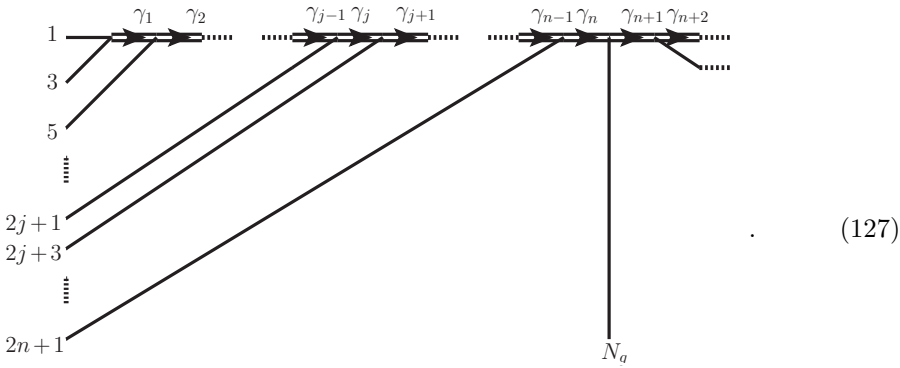
i.e. a blob with any number of legs, where one leg radiates a gluon.

4.1 Basis vector radiating gluon

In this section the colour structure of gluon radiation from basis vectors are evaluated. The starting colour structure is one of the basis vectors for $N_g - 1$ gluons that radiates a gluon from one leg



The legs in the basis vectors are numbered such that all odd numbers are on the left side and all even numbers on the right side, ascending reading downwards. For the radiated gluon this means that it should be last on the left side if $N_g = 2n + 3$ and last on the right side if $N_g = 2n + 2$. The idea is to rewrite eq. (126) as a sum over basis vectors for N_g gluons,



The constraints mentioned after eq. (128) and (129) give

$$\gamma_k \in (\beta_k \otimes A, \gamma_{k-1} \otimes A) \quad (132)$$

and comparing with eq. (127)

$$\begin{aligned} \gamma_l &= \beta_l, \quad \text{for } l = 1, \dots, j-1 \\ \gamma_{l+1} &= \beta_l, \quad \text{for } l = n, \dots, N_g - 3 \end{aligned} \quad (133)$$

where $N_g - 3$ comes from n being the number of gluons on the left side minus 1 (put gluon 1 and 3 into the common representation β_1 , every additional gluon gives one more representation), similarly on the right side, the number of gluons minus 1. The number of gluons on the left plus the number on the right is equal to N_g , hence $N_g - 2$, the additional -1 comes from all the gluons on the left side being in the same representation as all the gluons on the right side. The equation for a gluon radiated from a leg on the right side is found similarly by applying the same two pieces, eq. (128) and (129). With successive applications of eq. (131) and the corresponding equation for a gluon radiated from a leg on the right side, one can find the colour structures of basis vectors that have radiated multiple gluons.

4.2 Projection on basis vectors

From eq. (131) along with eq. (132) and (133) it can be seen that a basis vector for N_g gluons with an extra gluon attached to one of its legs is a sum of a small fraction of the basis vectors for $N_g + 1$ gluons, since many of the representations in the $N_g + 1$ vectors must be the same as in the N_g vector. From the first part of eq. (132) it is obvious that the closer to the middle the extra gluon is attached the more constrained the basis vectors with non-zero projection are, as more of their representations are constrained.

One can make an overestimate of the number of possible basis vectors on the right-hand side of eq. (131) for a given number of colours by using the result of the end of section 2.4 that there are at most $N_{\max} = N_c^2 - 1$ representations in $M \otimes A$. So every sum in eq. (131) can be over at most N_{\max} representations, i.e. the number of basis vectors with a non-zero coefficient are less than or equal to N_{\max}^{n-j+1} . As the constraints in eq. (132) are not taken into account this will be a bad overestimate. The number of basis vectors projected on, counted using the constraints of eq. (132), are given in table 5, along with the total number of basis vectors for comparison.

5 Conclusions and outlook

This thesis explores the decomposition of colour structures into a certain type of bases in colour space, the multiplet bases. Such bases have two very useful properties, orthogonality and minimality. This makes it possible to efficiently square the amplitudes involving more external partons, for which the colour space has a high dimensionality. The trade off, as compared to the commonly used bases, is a more complex basis decomposition, which is the subject of this thesis.

In section 2 interesting properties of the representations in the tensor product $A^{\otimes n_g}$ are derived. One of these properties is the first occurrence, which is the smallest n_g for

Table 5: Number of basis vectors projected on.

	N_g	6	8	10
Vectors	$N_c \geq N_g$	265	14,833	1,334,961
	QCD	145	3,598	107,160
Max	$N_c \geq N_g$	44	400	4,006
	QCD	33	178	962
Avg	$N_c \geq N_g$	18.8	80	429
	QCD	13.7	43	146

which a representation occurs in $A^{\otimes n_g}$, and has been found in [11]. Another property is an easy method of constructing all different representations in $A^{\otimes n_g}$, for any N_c . It turns out that the number of unique representations in $A^{\otimes n_g}$ grows slowly with the number of external partons, only as $\sim n_g^2$ for QCD (see eq. (77)). For general N_c , i.e. $N_c \geq N_g$, the scaling is exponential instead (eq. (73) and (74)). In doing this, a finite sum formula for the partition function P has been derived, see appendix A.

A method of decomposing a colour structure into multiplet bases was described in section 3. The weights for the different multiplet basis vectors, as in eq. (48), are rewritten in terms of smaller vacuum bubbles, the $3j$ and $6j$ Wigner coefficients. These smaller vacuum bubbles can be evaluated and stored once and for all. A colour structure can then be evaluated by being rewritten in terms of the Wigner $3j$ and $6j$ coefficients and their stored values being used. One interesting point of this is the number of smaller bubbles that have to be calculated. This number scales well, the reason for this is the slow growth of the number of unique representations in $A^{\otimes n_g}$. In eq. (105) an upper limit for the number of required Wigner coefficients for QCD is given, which scales only quadratically in the number of external gluons. Table 4 lists the number of required Wigner coefficients. Even the number of Wigner coefficients for the large N_c limit stays relatively small for up to 12 external gluons. These numbers could be further reduced by application of the symmetries of eq. (110) and (111). In the appendix C all of the required Wigner $6j$ coefficients are listed for up to 6 external gluons.

A possibility for further study, is examining how many possible non-zero terms there are for the Feynman diagrams. For some Feynman diagrams the loops that have to be picked in order to reduce the number of vertices in the vacuum bubble are long. This results in more summations over representations, i.e. more terms have to be added together to find the weight for the basis vectors. It is of interest to know how many terms have to be added together for the worst Feynman diagrams and for the average diagram.

Another very interesting part of this thesis is the subject of section 4, relating basis vectors for $N_g - 1$ gluons that radiate one more gluon to the basis vectors for N_g gluons. Using eq. (131) and the corresponding equation for gluons radiated from legs on the right side and the Wigner coefficients in appendix C, it is possible to determine the radiation matrices for $5g$ to $6g$, this has been done in [25]. Another aspect of section 4 is the viability of this for many external gluons, how many basis vectors do the radiating

basis vectors project on? This has been calculated in table 5, for both the worst case and the average. The radiating $N_g - 1$ basis vectors only have a non-zero projection on a very small fraction of the N_g basis vectors. The results of section 4 could be applied to parton showers and for recursion relations for amplitudes. The application of the results on recursion relations is currently explored in collaboration with Y.-J. Du and M. Sjö Dahl.

Appendices

A Proof of finite sum formula for the partition function P

The number of different ways of writing an integer n as positive integers less than or equal to k , where the order is irrelevant, is $P(n, k)$. As an example there are 4 ways of writing the number 4 with integers less than or equal to 3,

$$4 = 1 + 1 + 1 + 1 = 1 + 1 + 2 = 2 + 2 = 1 + 3. \quad (134)$$

Hence the partition function $P(4, 3) = 4$. $P(n, 1) = 1$ for any n , since it can only be written as the addition of n 1s.

Assume $P(n, k-1)$ is known for all n . Using a similar notation as for quark diagrams of section 2.6.2, i.e. a specific way of writing an integer n is

$$n = 1 \cdot \alpha_1 + \dots + (k-1) \cdot \alpha_{k-1} \leftrightarrow (\alpha_1, \dots, \alpha_{k-1} |. \quad (135)$$

The α_i indices are then how many times the integer i occurs in that specific partitioning of n . The partitionings of n are just all different combinations of $\alpha_1, \dots, \alpha_{k-1}$ under the constraint $\sum_{i=1}^{k-1} i\alpha_i = n$. To find how $P(n, k)$ relates to $P(n', k-1)$, the number of different ways of partitioning $n - ik$ for all positive integers i such that $n - ik \geq 0$ are added.

The number of ways of picking α_i in $(\alpha_1, \dots, \alpha_{k-1}, 0 |$ with the condition that $\sum_{i=1}^{k-1} i\alpha_i = n$ is $P(n, k-1)$. For the partitions with one integer being k , i.e. $(\alpha'_1, \dots, \alpha'_{k-1}, 1 |$ with $\sum_{i=1}^{k-1} i\alpha'_i = n - k$ there are $P(n - k, k-1)$ possible partitions. In general the number of possible $(\alpha_1, \dots, \alpha_{k-1}, j |$ under the constraint $\sum_{i=1}^{k-1} i\alpha_i = n - jk$ are $P(n - jk, k-1)$, where $j = 0, 1, \dots, \lfloor \frac{n}{k} \rfloor$, adding all of them together is then

$$P(n, k) = \sum_{j=0}^{\lfloor \frac{n}{k} \rfloor} P(n - jk, k-1). \quad (136)$$

This relation can now be applied recursively until $P(n, k)$ is expressed only in terms of $P(n, 1) = 1$, doing this gives

$$P(n, k) = \sum_{i_k=0}^{\lfloor \frac{n}{k} \rfloor} \sum_{i_{k-1}=0}^{\lfloor \frac{n-i_k k}{k-1} \rfloor} \dots \sum_{i_2=0}^{\lfloor \frac{n-i_k k - i_{k-1}(k-1) - \dots - i_3 3}{2} \rfloor} 1. \quad (137)$$

Table 6: Changed basis vectors.

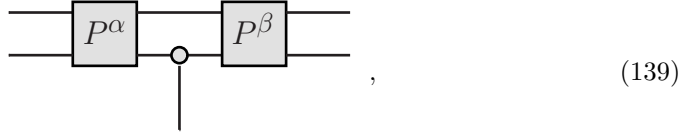
Number	α_1	α_3	α_2
197/203	8	0	$\overline{10}$
209	10	0	$\overline{10}$
212/213	$\overline{10}$	0	8
214	$\overline{10}$	0	10
216/217	$\overline{10}$	0	0
221/227	0	0	$\overline{10}$

The partition function $P(n) = P(n, n)$ is then

$$P(n) = \sum_{i_n=0}^{\lfloor \frac{n}{n} \rfloor} \sum_{i_{n-1}=0}^{\lfloor \frac{n-i_n n}{n-1} \rfloor} \dots \sum_{i_2=0}^{\lfloor \frac{n-i_n n - i_{n-1}(n-1) - \dots - i_3 3}{2} \rfloor} 1. \quad (138)$$

B Basis vectors for 6 external gluons

The sign of some of the basis vectors were changed in order to be consistent with the vertices being defined as



for representations with $n_f = 2$. The blob is in general a linear combination of f and d triple-gluon vertices, and is specified in [11]. The vectors that were changed are shown in table 6, where the first column specifies the vectors number in the list of vectors from [11]. The rows with two numbers are those where there are two possible vertices, for example the first row can have both the symmetric octet vertex or the antisymmetric, and both needed their sign to be changed.

C Wigner coefficients for 6 external gluons

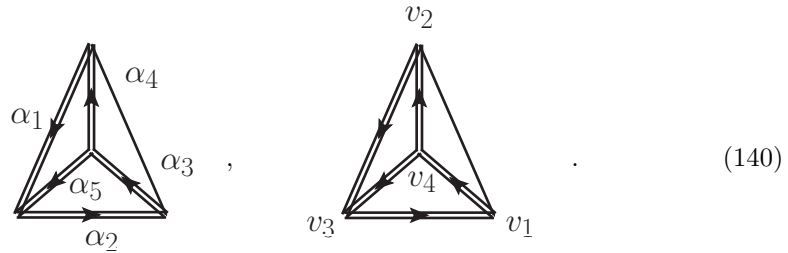
This section contains the required Wigner coefficients for 6 external gluons or for the radiation matrices for 5 to 6 external gluons. It assumes no loop like eq. (88) has been chosen (see section 3.4.1). The symmetries of eq. (110) and (111) have not been used to reduce the number of coefficients.

The representations are denoted by numbers for compactness, table C.1 contains translation from the numbers to the representations. To denote the Wigner coefficients the representations and vertices are specified as $\{\{\alpha_1, \alpha_2, 2, \alpha_3, \alpha_4, \alpha_5\}, \{v_1, v_2, v_3, v_4\}\}$

Table C.1: Numbering shorthand for representations.

Number	Representation	$SU(3)$ dim.
1	$(0 0)$	1
2	$(1 1)$	8
3	$(0, 1 1, 0)$	0
4	$(0, 1 2)$	$\overline{10}$
5	$(2 1, 0)$	10
6	$(2 2)$	27
7	$(0, 0, 1 1, 0, 0)$	0
8	$(0, 0, 1 1, 1)$	0
9	$(0, 0, 1 3)$	0
10	$(1, 1 1, 0, 0)$	0
11	$(1, 1 1, 1)$	0
12	$(1, 1 3)$	35bar
13	$(3 1, 0, 0)$	0
14	$(3 1, 1)$	35
15	$(3 3)$	64

(the 2 to denote the representation that is always an octet in the following coefficients),



The vertices, v_i , are 0 if the two representations are different since there is only one vertex for them (see section 2.4), and s or a if they are the same representation and symmetric or antisymmetric, respectively. The required Wigner $6j$ coefficients are in table C.2.

Table C.2: Required Wigner $6j$ coefficients on the form of eq. (140).

Representations and vertices	Value
$\{\{2,1,2,2,2,2\},\{0,a,0,s\}\}$	0
$\{\{2,1,2,2,2,2\},\{0,a,0,a\}\}$	$-\frac{1}{1-N_c^2}$
$\{\{2,2,2,2,2,2\},\{s,a,s,s\}\}$	0
$\{\{2,2,2,2,2,2\},\{s,a,s,a\}\}$	$-\frac{1}{2-2N_c^2}$
$\{\{2,2,2,2,2,2\},\{s,a,a,a\}\}$	0
$\{\{2,2,2,2,2,3\},\{s,a,0,0\}\}$	0
$\{\{2,2,2,2,2,4\},\{s,a,0,0\}\}$	$\frac{1}{\sqrt{N_c^2-4(N_c^2-1)}}$
$\{\{2,2,2,2,2,6\},\{s,a,0,0\}\}$	0
$\{\{2,2,2,2,2,2\},\{a,a,a,a\}\}$	$\frac{2(N_c^2-1)}{1}$
$\{\{2,2,2,2,2,3\},\{a,a,0,0\}\}$	$-\frac{1}{N_c-N_c^3}$
$\{\{2,2,2,2,2,4\},\{a,a,0,0\}\}$	0
$\{\{2,2,2,2,2,6\},\{a,a,0,0\}\}$	$\frac{1}{N_c-N_c^3}$
$\{\{2,2,2,3,2,3\},\{0,a,0,s\}\}$	0
$\{\{2,2,2,3,2,3\},\{0,a,0,a\}\}$	$\frac{\sqrt{2-\frac{6}{N_c}}}{(N_c-3)N_c(N_c+1)}$
$\{\{2,2,2,3,2,4\},\{0,a,0,0\}\}$	$-\frac{1}{\sqrt{N_c^2-3N_c+2(N_c^2+N_c)}}$
$\{\{2,2,2,3,2,5\},\{0,a,0,0\}\}$	$\frac{1}{\sqrt{N_c^2-3N_c+2(N_c^2+N_c)}}$
$\{\{2,2,2,4,2,4\},\{0,a,0,s\}\}$	0
$\{\{2,2,2,4,2,4\},\{0,a,0,a\}\}$	$\frac{\sqrt{2}}{\sqrt{N_c^2-4(N_c^2-1)}}$
$\{\{2,2,2,4,2,6\},\{0,a,0,0\}\}$	$-\frac{1}{(N_c-N_c^2)\sqrt{N_c^2+3N_c+2}}$
$\{\{2,2,2,5,2,6\},\{0,a,0,0\}\}$	$-\frac{1}{(N_c-1)N_c\sqrt{(N_c+1)(N_c+2)}}$
$\{\{2,2,2,6,2,6\},\{0,a,0,s\}\}$	0
$\{\{2,2,2,6,2,6\},\{0,a,0,a\}\}$	$\frac{\sqrt{\frac{6}{N_c}+2}}{(N_c-1)N_c(N_c+3)}$
$\{\{2,3,2,3,2,3\},\{s,a,s,s\}\}$	0
$\{\{2,3,2,3,2,3\},\{s,a,s,a\}\}$	$\frac{1}{\sqrt{2-\frac{6}{N_c}N_c(N_c^2-1)}}$
$\{\{2,3,2,3,2,3\},\{s,a,a,a\}\}$	0
$\{\{2,3,2,3,2,4\},\{s,a,0,0\}\}$	$-\frac{\sqrt{\frac{N_c^3-5N_c^2-2N_c+24}{N_c-2}}}{\sqrt{2}(N_c^4-N_c^3-7N_c^2+N_c+6)}$
$\{\{2,3,2,3,2,7\},\{s,a,0,0\}\}$	0
$\{\{2,3,2,3,2,8\},\{s,a,0,0\}\}$	$\frac{3\sqrt{N_c^4-7N_c^3+8N_c^2+28N_c-48}}{\sqrt{2}N_c(N_c^2-1)(N_c^3-5N_c^2-2N_c+24)}$
$\{\{2,3,2,3,2,11\},\{s,a,0,0\}\}$	0
$\{\{2,3,2,3,2,3\},\{a,a,a,a\}\}$	$\frac{1}{\sqrt{2}\sqrt{(N_c-3)N_c(N_c^2-1)}}$
$\{\{2,3,2,3,2,4\},\{a,a,0,0\}\}$	$\frac{(N_c-2)\sqrt{N_c(N_c^2-2N_c-3)}}{\sqrt{2}(N_c-3)(N_c-1)N_c^2(N_c+1)^{3/2}}$
$\{\{2,3,2,3,2,7\},\{a,a,0,0\}\}$	$\frac{2\sqrt{2}}{\sqrt{N_c-3}N_c^{3/2}(N_c-1)}$

Continued on next page

Table C.2 – continued from previous page

Representations and vertices	Value
$\{\{2,3,2,3,2,8\},\{a,a,0,0\}\}$	$\frac{1}{\sqrt{2}\sqrt{N_c-3}N_c^{3/2}(N_c^2-1)}$
$\{\{2,3,2,3,2,11\},\{a,a,0,0\}\}$	$-\frac{\sqrt{2}\sqrt{N_c^3-3N_c^2-N_c+3}}{(N_c-3)(N_c(N_c^2-1))^{3/2}}$
$\{\{2,3,2,4,2,4\},\{0,a,0,s\}\}$	$-\frac{\sqrt{N_c^4-13N_c^2+36}}{\sqrt{2}N_c(N_c^4-N_c^3-7N_c^2+N_c+6)}$
$\{\{2,3,2,4,2,4\},\{0,a,0,a\}\}$	$\frac{\sqrt{N_c^2-4}}{\sqrt{2}(N_c-2)N_c(N_c^2-1)}$
$\{\{2,3,2,4,2,8\},\{0,a,0,0\}\}$	$-\frac{\sqrt{3}\sqrt{N_c^2-N_c-6}}{N_c(N_c^4-N_c^3-7N_c^2+N_c+6)}$
$\{\{2,3,2,4,2,11\},\{0,a,0,0\}\}$	$-\frac{\sqrt{3}}{\sqrt{N_c^2-N_c-6}(N_c-N_c^3)}$
$\{\{2,3,2,5,2,10\},\{0,a,0,0\}\}$	$\frac{\sqrt{3}\sqrt{N_c^2-N_c-6}}{N_c(N_c^4-N_c^3-7N_c^2+N_c+6)}$
$\{\{2,3,2,5,2,11\},\{0,a,0,0\}\}$	$\frac{\sqrt{3}}{\sqrt{N_c^2-N_c-6}(N_c-N_c^3)}$
$\{\{2,4,2,4,2,4\},\{s,a,s,s\}\}$	$\frac{\sqrt{2}}{(N_c^2-1)\sqrt{N_c^4-13N_c^2+36}}$
$\{\{2,4,2,4,2,4\},\{s,a,s,a\}\}$	$\frac{\sqrt{N_c^4-5N_c^2+4}}{\sqrt{2}(N_c^2-4)(N_c^2-1)^{3/2}}$
$\{\{2,4,2,4,2,4\},\{s,a,a,a\}\}$	0
$\{\{2,4,2,4,2,6\},\{s,a,0,0\}\}$	$\frac{\sqrt{N_c^6-14N_c^4+49N_c^2-36}}{\sqrt{2}N_c(N_c^2-1)^{3/2}(N_c^2+N_c-6)}$
$\{\{2,4,2,4,2,8\},\{s,a,0,0\}\}$	$\frac{\sqrt{N_c^6-14N_c^4+49N_c^2-36}}{\sqrt{2}(N_c-3)N_c(N_c^2-4)(N_c^2-1)^{3/2}}$
$\{\{2,4,2,4,2,9\},\{s,a,0,0\}\}$	$\frac{2\sqrt{2}}{(N_c^2-1)\sqrt{N_c^4-13N_c^2+36}}$
$\{\{2,4,2,4,2,11\},\{s,a,0,0\}\}$	$-\frac{\sqrt{2}}{(N_c^2-1)\sqrt{N_c^4-13N_c^2+36}}$
$\{\{2,4,2,4,2,12\},\{s,a,0,0\}\}$	$\frac{\sqrt{N_c^6-14N_c^4+49N_c^2-36}}{\sqrt{2}N_c(N_c+3)(N_c^2-4)(N_c^2-1)^{3/2}}$
$\{\{2,4,2,4,2,4\},\{a,a,a,a\}\}$	$\frac{\sqrt{N_c^4-5N_c^2+4}}{\sqrt{2}(N_c^2-4)(N_c^2-1)^{3/2}}$
$\{\{2,4,2,4,2,6\},\{a,a,0,0\}\}$	$\frac{\sqrt{N_c^2-4}}{\sqrt{2}N_c(N_c+2)(N_c^2-1)}$
$\{\{2,4,2,4,2,8\},\{a,a,0,0\}\}$	$\frac{3\sqrt{N_c^2-4}}{\sqrt{2}(N_c^2-5N_c^3+4N_c)}$
$\{\{2,4,2,4,2,9\},\{a,a,0,0\}\}$	0
$\{\{2,4,2,4,2,11\},\{a,a,0,0\}\}$	0
$\{\{2,4,2,4,2,12\},\{a,a,0,0\}\}$	$\frac{3}{\sqrt{2}\sqrt{N_c^2-4}(N_c-N_c^3)}$
$\{\{2,4,2,6,2,6\},\{0,a,0,s\}\}$	$\frac{\sqrt{\frac{N_c+4}{N_c^3+3N_c^2-4N_c-12}}}{\sqrt{2}(N_c^2-1)}$
$\{\{2,4,2,6,2,6\},\{0,a,0,a\}\}$	$\frac{(N_c+2)\sqrt{N_c(N_c^2+2N_c-3)}}{\sqrt{2}(N_c-1)^{3/2}N_c^2(N_c+1)(N_c+3)}$
$\{\{2,4,2,6,2,11\},\{0,a,0,0\}\}$	$\frac{\sqrt{3}\sqrt{N_c^4+N_c^3-7N_c^2-N_c+6}}{N_c(N_c^2-1)^{3/2}(N_c^2+N_c-6)}$
$\{\{2,4,2,6,2,12\},\{0,a,0,0\}\}$	$-\frac{\sqrt{3}\sqrt{N_c^4+N_c^3-7N_c^2-N_c+6}}{N_c(N_c^2-1)^{3/2}(N_c^2+N_c-6)}$
$\{\{2,6,2,4,2,11\},\{0,a,0,0\}\}$	$\frac{\sqrt{3}\sqrt{N_c^4+N_c^3-7N_c^2-N_c+6}}{N_c(N_c^2-1)^{3/2}(N_c^2+N_c-6)}$

Continued on next page

Table C.2 – continued from previous page

Representations and vertices	Value
$\{\{2,6,2,4,2,12\},\{0,a,0,0\}\}$	$-\frac{\sqrt{3}\sqrt{N_c^4+N_c^3-7N_c^2-N_c+6}}{N_c(N_c^2-1)^{3/2}(N_c^2+N_c-6)}$
$\{\{2,6,2,6,2,6\},\{s,a,s,s\}\}$	0
$\{\{2,6,2,6,2,6\},\{s,a,s,a\}\}$	$\frac{1}{\sqrt{2}\sqrt{N_c(N_c+3)(N_c^2-1)}}$
$\{\{2,6,2,6,2,6\},\{s,a,a,a\}\}$	0
$\{\{2,6,2,6,2,11\},\{s,a,0,0\}\}$	0
$\{\{2,6,2,6,2,12\},\{s,a,0,0\}\}$	$\frac{3\sqrt{(N_c+2)(N_c^5+5N_c^4-3N_c^3-29N_c^2+2N_c+24)}}{\sqrt{2}N_c(N_c+3)(N_c^2-1)^{3/2}(N_c^2+2N_c-8)}$
$\{\{2,6,2,6,2,15\},\{s,a,0,0\}\}$	0
$\{\{2,6,2,6,2,6\},\{a,a,a,a\}\}$	$\frac{1}{\sqrt{2}\sqrt{N_c(N_c+3)(N_c^2-1)}}$
$\{\{2,6,2,6,2,11\},\{a,a,0,0\}\}$	$\frac{\sqrt{2}\sqrt{N_c^3+3N_c^2-N_c-3}}{(N_c+3)(N_c(N_c^2-1))^{3/2}}$
$\{\{2,6,2,6,2,12\},\{a,a,0,0\}\}$	$-\frac{\sqrt{N_c^3+3N_c^2-N_c-3}}{\sqrt{2}(N_c+3)(N_c(N_c^2-1))^{3/2}}$
$\{\{2,6,2,6,2,15\},\{a,a,0,0\}\}$	$-\frac{2\sqrt{2}}{N_c^{3/2}\sqrt{N_c+3}(N_c^2-1)}$
$\{\{2,1,2,2,1,2\},\{0,0,0,0\}\}$	$\frac{1}{N_c^2-1}$
$\{\{2,1,2,2,2,2\},\{0,a,0,s\}\}$	0
$\{\{2,2,2,1,2,2\},\{0,s,s,0\}\}$	$\frac{1}{N_c^2-1}$
$\{\{2,2,2,1,2,2\},\{0,a,a,0\}\}$	$-\frac{1}{1-N_c^2}$
$\{\{2,2,2,2,2,2\},\{s,s,s,s\}\}$	$\frac{N_c^2-12}{2(N_c^4-5N_c^2+4)}$
$\{\{2,2,2,2,2,2\},\{s,a,s,s\}\}$	0
$\{\{2,2,2,2,2,2\},\{s,a,a,s\}\}$	$-\frac{1}{2-2N_c^2}$
$\{\{2,2,2,2,2,2\},\{a,a,s,s\}\}$	$-\frac{1}{2-2N_c^2}$
$\{\{2,2,2,2,2,2\},\{a,a,a,s\}\}$	0
$\{\{2,2,2,2,2,2\},\{a,a,a,a\}\}$	$\frac{1}{2(N_c^2-1)}$
$\{\{3,2,2,1,2,2\},\{0,0,0,0\}\}$	$\frac{1}{N_c^2-1}$
$\{\{3,2,2,2,2,2\},\{s,0,0,s\}\}$	$-\frac{1}{(N_c-2)(N_c^2-1)}$
$\{\{3,2,2,2,2,2\},\{s,0,0,a\}\}$	0
$\{\{3,2,2,2,2,2\},\{a,0,0,a\}\}$	$-\frac{1}{N_c-N_c^3}$
$\{\{3,2,2,2,3,2\},\{s,s,0,0\}\}$	$\frac{\sqrt{2}\sqrt{N_c^2-7N_c+12}}{N_c(N_c^3-4N_c^2+N_c+6)}$
$\{\{3,2,2,2,3,2\},\{s,a,0,0\}\}$	0
$\{\{3,2,2,2,3,2\},\{a,s,0,0\}\}$	0
$\{\{3,2,2,2,3,2\},\{a,a,0,0\}\}$	$\frac{\sqrt{2}}{\sqrt{N_c-3}N_c^{3/2}(N_c+1)}$
$\{\{3,2,2,3,2,2\},\{0,0,0,0\}\}$	$\frac{N_c^2-N_c+2}{N_c^2(N_c^2-3N_c+2)(N_c^2-2N_c-3)}$
$\{\{3,2,2,3,3,2\},\{0,a,0,s\}\}$	0
$\{\{3,3,2,2,3,2\},\{0,s,s,0\}\}$	$\frac{2}{N_c^4-4N_c^3+N_c^2+6N_c}$
$\{\{3,3,2,2,3,2\},\{0,a,a,0\}\}$	$\frac{N_c^2(N_c^2-2N_c-3)}{2}$
$\{\{3,3,2,3,3,2\},\{s,s,s,s\}\}$	$\frac{3N_c^4-16N_c^3-12N_c^2+80N_c-64}{(N_c-2)N_c^2(N_c^2-2N_c-3)(N_c^3-3N_c^2-6N_c+8)}$

Continued on next page

Table C.2 – continued from previous page

Representations and vertices	Value
$\{\{3,3,2,3,3,2\},\{s,a,s,s\}\}$	0
$\{\{3,3,2,3,3,2\},\{s,a,a,s\}\}$	$\frac{1}{N_c(N_c^3-3N_c^2-N_c+3)}$
$\{\{3,3,2,3,3,2\},\{a,a,s,s\}\}$	$\frac{3N_c-4}{(N_c-1)N_c^2(N_c^2-2N_c-3)}$
$\{\{3,3,2,3,3,2\},\{a,a,a,s\}\}$	0
$\{\{3,3,2,3,3,2\},\{a,a,a,a\}\}$	$\frac{3N_c-4}{(N_c-1)N_c^2(N_c^2-2N_c-3)}$
$\{\{4,2,2,1,2,2\},\{0,0,0,0\}\}$	$-\frac{1}{1-N_c^2}$
$\{\{4,2,2,2,2,2\},\{s,0,0,s\}\}$	$-\frac{2}{N_c^4-5N_c^2+4}$
$\{\{4,2,2,2,2,2\},\{s,0,0,a\}\}$	$-\frac{1}{\sqrt{N_c^2-4}(N_c^2-1)}$
$\{\{4,2,2,2,2,2\},\{a,0,0,s\}\}$	$\frac{1}{\sqrt{N_c^2-4}(N_c^2-1)}$
$\{\{4,2,2,2,2,2\},\{a,0,0,a\}\}$	0
$\{\{4,2,2,2,3,2\},\{s,0,0,0\}\}$	$\frac{(N_c+2)\sqrt{N_c^3-2N_c^2-N_c+2}}{(N_c-1)(N_c^3+N_c^2-4N_c-4)^{3/2}}$
$\{\{4,2,2,2,3,2\},\{a,0,0,0\}\}$	$-\frac{1}{\sqrt{N_c^2-3N_c+2}(N_c^2+N_c)}$
$\{\{4,2,2,2,4,2\},\{s,s,0,0\}\}$	$\frac{\sqrt{2}\sqrt{N_c^4-10N_c^2+9}}{(N_c^2-4)(N_c^2-1)^{3/2}}$
$\{\{4,2,2,2,4,2\},\{s,a,0,0\}\}$	$-\frac{\sqrt{2}}{N_c^4-5N_c^2+4}$
$\{\{4,2,2,2,4,2\},\{a,s,0,0\}\}$	0
$\{\{4,2,2,2,4,2\},\{a,a,0,0\}\}$	$\frac{\sqrt{2}}{\sqrt{N_c^2-4}(N_c^2-1)}$
$\{\{4,2,2,3,2,2\},\{0,0,0,0\}\}$	$-\frac{1}{N_c^4-2N_c^3-N_c^2+2N_c}$
$\{\{4,2,2,3,3,2\},\{0,0,0,s\}\}$	$-\frac{\sqrt{2}\sqrt{\frac{N_c-4}{N_c^3-2N_c^2-5N_c+6}}}{(N_c-2)N_c(N_c+1)}$
$\{\{4,2,2,3,3,2\},\{0,0,0,a\}\}$	$\frac{\sqrt{2}\sqrt{\frac{N_c^3-6N_c^2+11N_c-6}{N_c^3}}}{N_c^4-5N_c^3+5N_c^2+5N_c-6}$
$\{\{4,2,2,3,4,2\},\{0,s,0,0\}\}$	$\frac{\sqrt{2}\sqrt{\frac{N_c^4-10N_c^2+9}{N_c+2}}}{(N_c-2)N_c(N_c+1)^{3/2}(N_c^2-4N_c+3)}$
$\{\{4,2,2,3,4,2\},\{0,a,0,0\}\}$	$-\frac{\sqrt{2}}{N_c(-N_c^2+N_c+2)\sqrt{N_c^2+N_c-2}}$
$\{\{4,2,2,4,2,2\},\{0,0,0,0\}\}$	$\frac{1}{N_c^4-5N_c^2+4}$
$\{\{4,2,2,4,4,2\},\{0,a,0,s\}\}$	0
$\{\{4,3,2,2,2,2\},\{0,0,0,s\}\}$	$\frac{\sqrt{\frac{N_c-1}{N_c+2}}}{N_c^3-2N_c^2-N_c+2}$
$\{\{4,3,2,2,2,2\},\{0,0,0,a\}\}$	$\frac{1}{\sqrt{N_c^2-3N_c+2}(N_c^2+N_c)}$
$\{\{4,3,2,2,3,2\},\{0,0,0,0\}\}$	$\frac{2}{N_c^2(N_c^3-4N_c^2+N_c+6)}$
$\{\{4,3,2,2,4,2\},\{0,s,0,0\}\}$	$\frac{\sqrt{2}\sqrt{\frac{N_c^3+4N_c^2+N_c-6}{N_c-3}}}{N_c^5-5N_c^3+4N_c}$
$\{\{4,3,2,2,4,2\},\{0,a,0,0\}\}$	$\frac{\sqrt{2}\sqrt{N_c^2+N_c-2}}{N_c^5-5N_c^3+4N_c}$
$\{\{4,3,2,3,2,2\},\{s,0,0,0\}\}$	$-\frac{\sqrt{2}\sqrt{\frac{N_c^2-7N_c+12}{N_c^2+N_c-2}}}{N_c(N_c^3-4N_c^2+N_c+6)}$

Continued on next page

Table C.2 – continued from previous page

Representations and vertices	Value
$\{\{4,3,2,3,2,2\},\{a,0,0,0\}\}$	$-\frac{\sqrt{2}}{N_c^2(N_c+1)\sqrt{N_c^2-6N_c-\frac{6}{N_c}+11}}$
$\{\{4,3,2,3,3,2\},\{s,0,0,s\}\}$	$-\frac{N_c^2-2N_c+4}{-N_c^6+3N_c^5+5N_c^4-15N_c^3-4N_c^2+12N_c}$
$\{\{4,3,2,3,3,2\},\{s,0,0,a\}\}$	$\frac{\sqrt{\frac{N_c^2-2N_c-8}{(N_c-2)N_c}}}{N_c^4-N_c^3-7N_c^2+N_c+6}$
$\{\{4,3,2,3,3,2\},\{a,0,0,s\}\}$	$-\frac{\sqrt{\frac{N_c^2-2N_c-8}{(N_c-2)N_c}}}{N_c^4-N_c^3-7N_c^2+N_c+6}$
$\{\{4,3,2,3,3,2\},\{a,0,0,a\}\}$	$\frac{2-N_c}{N_c^2(N_c^3-3N_c^2-N_c+3)}$
$\{\{4,3,2,3,4,2\},\{s,s,0,0\}\}$	$\frac{\sqrt{(N_c-4)(N_c+3)(3N_c-4)}}{(N_c-3)(N_c-2)(N_c-1)N_c(N_c+1)(N_c+2)}$
$\{\{4,3,2,3,4,2\},\{s,a,0,0\}\}$	$\frac{\sqrt{N_c^2-7N_c+12}}{N_c^5-3N_c^4-5N_c^3+15N_c^2+4N_c-12}$
$\{\{4,3,2,3,4,2\},\{a,s,0,0\}\}$	$\frac{(N_c-2)\sqrt{\frac{N_c+3}{N_c^2-4}}}{(N_c-3)(N_c-1)N_c^{3/2}(N_c+1)}$
$\{\{4,3,2,3,4,2\},\{a,a,0,0\}\}$	$\frac{(3N_c-2)\sqrt{\frac{N_c^2-N_c-6}{N_c-2}}}{(N_c-3)(N_c-1)N_c^{3/2}(N_c+1)(N_c+2)}$
$\{\{4,3,2,4,2,2\},\{0,0,0,0\}\}$	$\frac{N_c^5-5N_c^3+4N_c}{2(N_c^3-2N_c^2-2N_c+2)}$
$\{\{4,3,2,4,3,2\},\{0,0,0,0\}\}$	$\frac{N_c^2(N_c^2-2N_c-3)(N_c^3-N_c^2-4N_c+4)}{N_c^5-5N_c^3+4N_c}$
$\{\{4,3,2,4,4,2\},\{0,a,0,s\}\}$	$-\frac{\sqrt{N_c^2-9}}{N_c(N_c^4-N_c^3-7N_c^2+N_c+6)}$
$\{\{4,4,2,2,4,2\},\{0,s,s,0\}\}$	$-\frac{2}{N_c^4-5N_c^2+4}$
$\{\{4,4,2,2,4,2\},\{0,a,s,0\}\}$	0
$\{\{4,4,2,2,4,2\},\{0,a,a,0\}\}$	$-\frac{2}{N_c^4-5N_c^2+4}$
$\{\{4,4,2,3,4,2\},\{0,s,s,0\}\}$	$\frac{N_c^2-3N_c+6}{(N_c-3)N_c(N_c^4-5N_c^2+4)}$
$\{\{4,4,2,3,4,2\},\{0,a,s,0\}\}$	$\frac{\sqrt{\frac{N_c+3}{N_c-3}}}{N_c(-N_c^3-2N_c^2+N_c+2)}$
$\{\{4,4,2,3,4,2\},\{0,a,a,0\}\}$	$-\frac{1}{N_c(N_c^3-2N_c^2-N_c+2)}$
$\{\{4,4,2,4,4,2\},\{s,s,s,s\}\}$	$\frac{3N_c^2-47}{(N_c^2-9)(N_c^4-5N_c^2+4)}$
$\{\{4,4,2,4,4,2\},\{s,a,s,s\}\}$	$-\frac{2\sqrt{N_c^6-14N_c^4+49N_c^2-36}}{(N_c^2-9)(N_c^4-5N_c^2+4)^{3/2}}$
$\{\{4,4,2,4,4,2\},\{s,a,a,s\}\}$	$-\frac{1}{N_c^4+5N_c^2-4}$
$\{\{4,4,2,4,4,2\},\{a,a,s,s\}\}$	$\frac{3}{N_c^4-5N_c^2+4}$
$\{\{4,4,2,4,4,2\},\{a,a,a,s\}\}$	0
$\{\{4,4,2,4,4,2\},\{a,a,a,a\}\}$	$\frac{3}{N_c^4-5N_c^2+4}$
$\{\{5,2,2,4,2,2\},\{0,0,0,0\}\}$	$\frac{1}{N_c^4-5N_c^2+4}$
$\{\{5,2,2,4,3,2\},\{0,0,0,0\}\}$	$\frac{2}{N_c(N_c+1)(N_c^2-4)}$
$\{\{5,3,2,4,2,2\},\{0,0,0,0\}\}$	$\frac{N_c(N_c^3+N_c^2-4N_c-4)}{2}$
$\{\{5,3,2,4,3,2\},\{0,0,0,0\}\}$	$-\frac{4}{N_c^2(N_c^2-4)(N_c^2-2N_c-3)}$
$\{\{6,2,2,1,2,2\},\{0,0,0,0\}\}$	$\frac{1}{N_c^2-1}$

Continued on next page

Table C.2 – continued from previous page

Representations and vertices	Value
$\{\{6,2,2,2,2,2\},\{s,0,0,s\}\}$	$\frac{1}{(N_c+2)(N_c^2-1)}$
$\{\{6,2,2,2,2,2\},\{s,0,0,a\}\}$	0
$\{\{6,2,2,2,2,2\},\{a,0,0,a\}\}$	$\frac{1}{N_c-N_c^3}$
$\{\{6,2,2,2,4,2\},\{s,0,0,0\}\}$	$\frac{1}{\sqrt{(N_c-2)(N_c+1)}(N_c^2+N_c-2)}$
$\{\{6,2,2,2,4,2\},\{a,0,0,0\}\}$	$\frac{\sqrt{\frac{N_c+1}{N_c+2}}}{N_c(N_c^2-1)}$
$\{\{6,2,2,2,5,2\},\{s,0,0,0\}\}$	$\frac{1}{\sqrt{(N_c-2)(N_c+1)}(N_c^2+N_c-2)}$
$\{\{6,2,2,2,5,2\},\{a,0,0,0\}\}$	$\frac{\sqrt{\frac{N_c+1}{N_c+2}}}{N_c-N_c^3}$
$\{\{6,2,2,2,6,2\},\{s,s,0,0\}\}$	$\frac{\sqrt{2}\sqrt{\frac{N_c+4}{N_c+3}}}{(N_c-1)N_c(N_c+2)}$
$\{\{6,2,2,2,6,2\},\{s,a,0,0\}\}$	0
$\{\{6,2,2,2,6,2\},\{a,s,0,0\}\}$	0
$\{\{6,2,2,2,6,2\},\{a,a,0,0\}\}$	$\frac{\sqrt{2}}{(N_c-1)N_c^{3/2}\sqrt{N_c+3}}$
$\{\{6,2,2,3,2,2\},\{0,0,0,0\}\}$	$\frac{1}{N_c^2(N_c^2-1)}$
$\{\{6,2,2,3,4,2\},\{0,0,0,0\}\}$	$-\frac{2}{N_c^2\sqrt{N_c^4-5N_c^2+4}}$
$\{\{6,2,2,3,5,2\},\{0,0,0,0\}\}$	$-\frac{2}{N_c^2\sqrt{N_c^4-5N_c^2+4}}$
$\{\{6,2,2,4,2,2\},\{0,0,0,0\}\}$	$-\frac{1}{(N_c-1)N_c(N_c+1)(N_c+2)}$
$\{\{6,2,2,4,4,2\},\{0,0,0,s\}\}$	$\frac{\sqrt{2}\sqrt{\frac{N_c^4-5N_c^3+5N_c^2+5N_c-6}{N_c+3}}}{(N_c-1)^{3/2}N_c(N_c^3+N_c^2-4N_c-4)}$
$\{\{6,2,2,4,4,2\},\{0,0,0,a\}\}$	$\frac{\sqrt{2}\sqrt{N_c^3-2N_c^2-N_c+2}}{(N_c-1)^{3/2}N_c(N_c^3+N_c^2-4N_c-4)}$
$\{\{6,2,2,4,6,2\},\{0,s,0,0\}\}$	$-\frac{\sqrt{2}\sqrt{\frac{N_c^2+7N_c+12}{(N_c-1)^2(N_c^2-N_c-2)}}}{N_c(N_c^2+5N_c+6)}$
$\{\{6,2,2,4,6,2\},\{0,a,0,0\}\}$	$\frac{\sqrt{2}}{(N_c-1)N_c^{3/2}\sqrt{(N_c+3)}(N_c^2+3N_c+2)}$
$\{\{6,2,2,5,5,2\},\{0,0,0,s\}\}$	$\frac{\sqrt{2}\sqrt{\frac{N_c^4-5N_c^3+5N_c^2+5N_c-6}{N_c+3}}}{(N_c-1)^{3/2}N_c(N_c^3+N_c^2-4N_c-4)}$
$\{\{6,2,2,5,5,2\},\{0,0,0,a\}\}$	$-\frac{\sqrt{2}\sqrt{N_c^3-2N_c^2-N_c+2}}{(N_c-1)^{3/2}N_c(N_c^3+N_c^2-4N_c-4)}$
$\{\{6,2,2,5,6,2\},\{0,s,0,0\}\}$	$-\frac{\sqrt{2}\sqrt{\frac{N_c^2+7N_c+12}{(N_c-1)^2(N_c^2-N_c-2)}}}{N_c(N_c^2+5N_c+6)}$
$\{\{6,2,2,5,6,2\},\{0,a,0,0\}\}$	$-\frac{\sqrt{2}}{(N_c-1)N_c^{3/2}\sqrt{(N_c+3)}(N_c^2+3N_c+2)}$
$\{\{6,2,2,6,2,2\},\{0,0,0,0\}\}$	$\frac{N_c^2+N_c+2}{N_c^2(N_c^2+2N_c-3)(N_c^2+3N_c+2)}$
$\{\{6,2,2,6,6,2\},\{0,a,0,s\}\}$	0
$\{\{6,4,2,2,4,2\},\{0,0,0,0\}\}$	$-\frac{2}{N_c^5-5N_c^3+4N_c}$
$\{\{6,4,2,2,5,2\},\{0,0,0,0\}\}$	$\frac{2(N_c+1)}{N_c(N_c^4-5N_c^2+4)}$
$\{\{6,4,2,3,4,2\},\{0,0,0,0\}\}$	$-\frac{4}{N_c^6-5N_c^4+4N_c^2}$
$\{\{6,4,2,3,5,2\},\{0,0,0,0\}\}$	$\frac{4}{N_c^2(N_c^2-4)}$

Continued on next page

Table C.2 – continued from previous page

Representations and vertices	Value
$\{\{6,4,2,4,4,2\},\{s,0,0,s\}\}$	$\frac{N_c^2+3N_c+6}{N_c(N_c+3)(N_c^4-5N_c^2+4)}$
$\{\{6,4,2,4,4,2\},\{s,0,0,a\}\}$	$-\frac{\sqrt{N_c^2-9}}{N_c^5+N_c^4-7N_c^3-N_c^2+6N_c}$
$\{\{6,4,2,4,4,2\},\{a,0,0,s\}\}$	$\frac{\sqrt{N_c^2-9}}{N_c^5+N_c^4-7N_c^3-N_c^2+6N_c}$
$\{\{6,4,2,4,4,2\},\{a,0,0,a\}\}$	$\frac{1}{-N_c^4-2N_c^3+N_c^2+2N_c}$
$\{\{6,4,2,4,6,2\},\{s,s,0,0\}\}$	$\frac{(3N_c+4)\sqrt{N_c^2+N_c-12}}{(N_c-2)(N_c-1)N_c(N_c+1)(N_c+2)(N_c+3)}$
$\{\{6,4,2,4,6,2\},\{s,a,0,0\}\}$	$-\frac{(N_c+2)\sqrt{\frac{(N_c-3)N_c}{N_c^2-4}}}{(N_c-1)N_c^2(N_c+1)(N_c+3)}$
$\{\{6,4,2,4,6,2\},\{a,s,0,0\}\}$	$-\frac{\sqrt{N_c^2+7N_c+12}}{N_c^5+3N_c^4-5N_c^3-15N_c^2+4N_c+12}$
$\{\{6,4,2,4,6,2\},\{a,a,0,0\}\}$	$\frac{3N_c+2}{N_c^{3/2}(N_c^2-1)\sqrt{N_c^3+3N_c^2-4N_c-12}}$
$\{\{6,4,2,6,2,2\},\{0,0,0,0\}\}$	$-\frac{N_c^2(N_c^3+4N_c^2+N_c-6)}{2(N_c^3+2N_c^2-2N_c-2)}$
$\{\{6,4,2,6,4,2\},\{0,0,0,0\}\}$	$\frac{N_c^2(N_c^2+2N_c-3)(N_c^3+N_c^2-4N_c-4)}{1}$
$\{\{6,4,2,6,6,2\},\{0,a,0,s\}\}$	$\frac{1}{(N_c-1)(N_c+1)(N_c+3)\sqrt{\frac{N_c(N_c^2-4)}{N_c+4}}}$
$\{\{6,5,2,2,4,2\},\{0,0,0,0\}\}$	$\frac{2}{(N_c-1)N_c(N_c^2-4)}$
$\{\{6,5,2,3,4,2\},\{0,0,0,0\}\}$	$\frac{4}{N_c^2(N_c^2-4)}$
$\{\{6,5,2,6,4,2\},\{0,0,0,0\}\}$	$-\frac{4}{N_c^2(N_c^2-4)(N_c^2+2N_c-3)}$
$\{\{6,5,2,6,6,2\},\{0,a,0,s\}\}$	$\frac{\sqrt{\frac{N_c+4}{N_c(N_c^2-4)}}}{-N_c^3-3N_c^2+N_c+3}$
$\{\{6,6,2,2,6,2\},\{0,s,s,0\}\}$	$\frac{N_c(N_c+2)(N_c^2+2N_c-3)}{2}$
$\{\{6,6,2,2,6,2\},\{0,a,a,0\}\}$	$\frac{N_c^2(N_c^2+2N_c-3)}{2}$
$\{\{6,6,2,4,6,2\},\{0,s,s,0\}\}$	$\frac{N_c^2+2N_c+4}{N_c^6+3N_c^5-5N_c^4-15N_c^3+4N_c^2+12N_c}$
$\{\{6,6,2,4,6,2\},\{0,a,a,0\}\}$	$\frac{N_c+2}{N_c^2(-N_c^3-3N_c^2+N_c+3)}$
$\{\{6,6,2,6,6,2\},\{s,s,s,s\}\}$	$\frac{3N_c^4+16N_c^3-12N_c^2-80N_c-64}{N_c^2(N_c^2+2N_c-3)(N_c^4+5N_c^3-20N_c-16)}$
$\{\{6,6,2,6,6,2\},\{s,a,s,s\}\}$	0
$\{\{6,6,2,6,6,2\},\{s,a,a,s\}\}$	$-\frac{1}{-N_c^4-3N_c^3+N_c^2+3N_c}$
$\{\{6,6,2,6,6,2\},\{a,a,s,s\}\}$	$\frac{3N_c+4}{N_c^2(N_c+1)(N_c^2+2N_c-3)}$
$\{\{6,6,2,6,6,2\},\{a,a,a,s\}\}$	0
$\{\{6,6,2,6,6,2\},\{a,a,a,a\}\}$	$\frac{3N_c+4}{N_c^2(N_c+1)(N_c^2+2N_c-3)}$
$\{\{7,3,2,2,3,2\},\{0,0,0,0\}\}$	$\frac{4}{(N_c-3)N_c^2(N_c+1)}$
$\{\{7,3,2,3,3,2\},\{s,0,0,s\}\}$	$-\frac{4}{(N_c-3)N_c(N_c+1)(N_c^2-5N_c+4)}$
$\{\{7,3,2,3,3,2\},\{s,0,0,a\}\}$	0
$\{\{7,3,2,3,3,2\},\{a,0,0,a\}\}$	$\frac{4}{(N_c-3)N_c^2(N_c^2-1)}$
$\{\{7,3,2,4,3,2\},\{0,0,0,0\}\}$	$\frac{4}{N_c^2(N_c^3-3N_c^2-N_c+3)}$
$\{\{7,3,2,7,3,2\},\{0,0,0,0\}\}$	$\frac{4(N_c^2-3N_c+8)}{(N_c-1)^2N_c^2(N_c^2-7N_c+12)(N_c^2-4N_c-5)}$

Continued on next page

Table C.2 – continued from previous page

Representations and vertices	Value
$\{\{8,3,2,2,3,2\},\{0,0,0,0\}\}$	$\frac{2}{(N_c-3)N_c^2(N_c+1)}$
$\{\{8,3,2,2,4,2\},\{0,0,0,0\}\}$	$\frac{2\sqrt{3}}{N_c(N_c+1)\sqrt{(N_c^2-4)(N_c^2-4N_c+3)}}$
$\{\{8,3,2,3,3,2\},\{s,0,0,s\}\}$	$-\frac{10-N_c}{(N_c-3)N_c(N_c+1)(N_c^3-3N_c^2-6N_c+8)}$
$\{\{8,3,2,3,3,2\},\{s,0,0,a\}\}$	$-\frac{3(N_c-2)}{(N_c-3)(N_c-1)N_c^2(N_c+1)\sqrt{N_c^2-4N_c+\frac{16}{N_c}-4}}$
$\{\{8,3,2,3,3,2\},\{a,0,0,s\}\}$	$\frac{3(N_c-2)}{(N_c-3)(N_c-1)N_c^2(N_c+1)\sqrt{N_c^2-4N_c+\frac{16}{N_c}-4}}$
$\{\{8,3,2,3,3,2\},\{a,0,0,a\}\}$	$-\frac{1}{N_c^2(N_c^3-3N_c^2-N_c+3)}$
$\{\{8,3,2,3,4,2\},\{s,0,0,0\}\}$	$-\frac{\sqrt{6}}{N_c\sqrt{N_c^2-6N_c+8(N_c^3-3N_c^2-N_c+3)}}$
$\{\{8,3,2,3,4,2\},\{a,0,0,0\}\}$	$\frac{\sqrt{6}}{N_c^{3/2}\sqrt{N_c+2(N_c^3-3N_c^2-N_c+3)}}$
$\{\{8,3,2,4,3,2\},\{0,0,0,0\}\}$	$\frac{N_c^2(N_c^3-3N_c^2-N_c+3)}{2}$
$\{\{8,3,2,4,4,2\},\{0,0,0,s\}\}$	$\frac{\sqrt{6}\sqrt{\frac{N_c+3}{N_c-2}}}{N_c(N_c^4-N_c^3-7N_c^2+N_c+6)}$
$\{\{8,3,2,4,4,2\},\{0,0,0,a\}\}$	$-\frac{\sqrt{6}}{N_c\sqrt{N_c^2-5N_c+6(-N_c^3-2N_c^2+N_c+2)}}$
$\{\{8,3,2,5,3,2\},\{0,0,0,0\}\}$	$-\frac{4}{N_c^2(N_c^3-7N_c-6)}$
$\{\{8,3,2,7,3,2\},\{0,0,0,0\}\}$	$-\frac{4}{(N_c-3)(N_c-1)N_c^2(N_c^2-3N_c-4)}$
$\{\{8,3,2,8,3,2\},\{0,0,0,0\}\}$	$\frac{2(2N_c^2-6N_c-5)}{N_c^2(N_c^2-4N_c+3)(N_c^4-3N_c^3-8N_c^2+12N_c+16)}$
$\{\{8,4,2,2,3,2\},\{0,0,0,0\}\}$	$\frac{2\sqrt{3}}{N_c(N_c+1)\sqrt{(N_c^2-4)(N_c^2-4N_c+3)}}$
$\{\{8,4,2,2,4,2\},\{0,0,0,0\}\}$	$-\frac{2}{N_c^4-5N_c^2+4}$
$\{\{8,4,2,3,3,2\},\{0,0,0,s\}\}$	$-\frac{\sqrt{6}}{N_c\sqrt{N_c^2-6N_c+8(N_c^3-3N_c^2-N_c+3)}}$
$\{\{8,4,2,3,3,2\},\{0,0,0,a\}\}$	$-\frac{\sqrt{6}}{N_c^{3/2}\sqrt{N_c+2(N_c^3-3N_c^2-N_c+3)}}$
$\{\{8,4,2,3,4,2\},\{0,0,0,0\}\}$	$\frac{2}{(N_c-3)(N_c-1)(N_c+1)(N_c^2-4)}$
$\{\{8,4,2,4,3,2\},\{s,0,0,0\}\}$	$\frac{\sqrt{6}\sqrt{\frac{N_c+3}{N_c-2}}}{N_c(N_c^4-N_c^3-7N_c^2+N_c+6)}$
$\{\{8,4,2,4,3,2\},\{a,0,0,0\}\}$	$-\frac{\sqrt{6}}{(N_c-1)N_c\sqrt{N_c^2-5N_c+6(N_c^2+3N_c+2)}}$
$\{\{8,4,2,4,4,2\},\{s,0,0,s\}\}$	$-\frac{3N_c^2+10N_c+3}{N_c(N_c^6-14N_c^4+49N_c^2-36)}$
$\{\{8,4,2,4,4,2\},\{s,0,0,a\}\}$	$\frac{\sqrt{N_c^2-9}}{(N_c-3)(N_c-1)N_c(N_c^3+N_c^2-4N_c-4)}$
$\{\{8,4,2,4,4,2\},\{a,0,0,s\}\}$	$-\frac{\sqrt{N_c^2-9}}{(N_c-3)(N_c-1)N_c(N_c^3+N_c^2-4N_c-4)}$
$\{\{8,4,2,4,4,2\},\{a,0,0,a\}\}$	$\frac{3}{N_c^5-5N_c^3+4N_c}$
$\{\{8,4,2,6,4,2\},\{0,0,0,0\}\}$	$\frac{4}{N_c^5-5N_c^3+4N_c}$
$\{\{8,4,2,8,3,2\},\{0,0,0,0\}\}$	$-\frac{18}{N_c^2(N_c^2-4N_c+3)(N_c^4-3N_c^3-8N_c^2+12N_c+16)}$
$\{\{8,4,2,8,4,2\},\{0,0,0,0\}\}$	$\frac{4N_c^2-4N_c+6}{N_c^2(N_c^2-4N_c+3)(N_c^4-3N_c^3-8N_c^2+12N_c+16)}$
$\{\{9,4,2,2,4,2\},\{0,0,0,0\}\}$	$-\frac{4}{N_c^4-5N_c^2+4}$
$\{\{9,4,2,3,4,2\},\{0,0,0,0\}\}$	$\frac{4}{(N_c^2-2N_c-3)(N_c^3-N_c^2-4N_c+4)}$

Continued on next page

Table C.2 – continued from previous page

Representations and vertices	Value
$\{\{9,4,2,4,4,2\},\{s,0,0,s\}\}$	$-\frac{8}{(N_c^2-9)(N_c^4-5N_c^2+4)}$
$\{\{9,4,2,4,4,2\},\{s,0,0,a\}\}$	$-\frac{\sqrt{N_c^2-9}(N_c^4-5N_c^2+4)}{4}$
$\{\{9,4,2,4,4,2\},\{a,0,0,s\}\}$	$\frac{\sqrt{N_c^2-9}(N_c^4-5N_c^2+4)}{4}$
$\{\{9,4,2,4,4,2\},\{a,0,0,a\}\}$	0
$\{\{9,4,2,6,4,2\},\{0,0,0,0\}\}$	$-\frac{4(N_c-3)}{N_c^6-14N_c^4+49N_c^2-36}$
$\{\{9,4,2,8,4,2\},\{0,0,0,0\}\}$	$-\frac{N_c(N_c^5-3N_c^4-5N_c^3+15N_c^2+4N_c-12)}{4}$
$\{\{9,4,2,9,4,2\},\{0,0,0,0\}\}$	$\frac{N_c^6-14N_c^4+49N_c^2-36}{4}$
$\{\{10,3,2,8,3,2\},\{0,0,0,0\}\}$	$\frac{N_c^2(N_c^4-4N_c^3-7N_c^2+22N_c+24)}{4}$
$\{\{11,3,2,2,3,2\},\{0,0,0,0\}\}$	$\frac{1}{(N_c-3)N_c^2(N_c+1)}$
$\{\{11,3,2,2,4,2\},\{0,0,0,0\}\}$	$-\frac{\sqrt{3}}{(N_c^2+N_c)\sqrt{N_c^4-4N_c^3-N_c^2+16N_c-12}}$
$\{\{11,3,2,2,5,2\},\{0,0,0,0\}\}$	$-\frac{\sqrt{3}}{(N_c^2+N_c)\sqrt{N_c^4-4N_c^3-N_c^2+16N_c-12}}$
$\{\{11,3,2,2,6,2\},\{0,0,0,0\}\}$	$\frac{3}{N_c^2\sqrt{N_c^4-10N_c^2+9}}$
$\{\{11,3,2,3,3,2\},\{s,0,0,s\}\}$	$\frac{2}{N_c(N_c^4-N_c^3-7N_c^2+N_c+6)}$
$\{\{11,3,2,3,3,2\},\{s,0,0,a\}\}$	0
$\{\{11,3,2,3,3,2\},\{a,0,0,a\}\}$	$-\frac{2}{N_c^2(N_c^3-3N_c^2-N_c+3)}$
$\{\{11,3,2,3,4,2\},\{s,0,0,0\}\}$	$-\frac{\sqrt{6}\sqrt{\frac{N_c^3-6N_c^2+5}{N_c-2}}\frac{N_c+12}{N_c-2}}{(N_c-1)N_c(N_c+2)(N_c^2-2N_c-3)^{3/2}}$
$\{\{11,3,2,3,4,2\},\{a,0,0,0\}\}$	$\frac{\sqrt{6}\sqrt{\frac{N_c+2}{N_c^3}}}{N_c^4-N_c^3-7N_c^2+N_c+6}$
$\{\{11,3,2,3,5,2\},\{s,0,0,0\}\}$	$-\frac{\sqrt{6}\sqrt{\frac{N_c^3-6N_c^2+5}{N_c-2}}\frac{N_c+12}{N_c-2}}{(N_c-1)N_c(N_c+2)(N_c^2-2N_c-3)^{3/2}}$
$\{\{11,3,2,3,5,2\},\{a,0,0,0\}\}$	$-\frac{\sqrt{6}\sqrt{\frac{N_c+2}{N_c^3}}}{N_c^4-N_c^3-7N_c^2+N_c+6}$
$\{\{11,3,2,4,3,2\},\{0,0,0,0\}\}$	$-\frac{2}{N_c^2(N_c^3-7N_c-6)}$
$\{\{11,3,2,4,4,2\},\{0,0,0,s\}\}$	$\frac{\sqrt{6}}{N_c(N_c+2)(N_c^2-1)\sqrt{N_c^2+N_c-6}}$
$\{\{11,3,2,4,4,2\},\{0,0,0,a\}\}$	$\frac{\sqrt{6}}{N_c(N_c+2)(N_c^2-1)\sqrt{N_c^2-5N_c+6}}$
$\{\{11,3,2,4,6,2\},\{0,0,0,0\}\}$	$-\frac{6}{(N_c^2-N_c^4)\sqrt{N_c^4-13N_c^2+36}}$
$\{\{11,3,2,5,5,2\},\{0,0,0,s\}\}$	$\frac{\sqrt{6}}{N_c(N_c+2)(N_c^2-1)\sqrt{N_c^2+N_c-6}}$
$\{\{11,3,2,5,5,2\},\{0,0,0,a\}\}$	$-\frac{\sqrt{6}}{N_c(N_c+2)(N_c^2-1)\sqrt{N_c^2-5N_c+6}}$
$\{\{11,3,2,5,6,2\},\{0,0,0,0\}\}$	$-\frac{6}{(N_c^2-N_c^4)\sqrt{N_c^4-13N_c^2+36}}$
$\{\{11,3,2,7,3,2\},\{0,0,0,0\}\}$	$\frac{4}{(N_c-1)^2N_c^2(N_c^2-2N_c-3)}$
$\{\{11,3,2,8,3,2\},\{0,0,0,0\}\}$	$-\frac{4}{N_c^2(N_c^4-N_c^3-7N_c^2+N_c+6)}$
$\{\{11,3,2,8,4,2\},\{0,0,0,0\}\}$	0
$\{\{11,3,2,10,5,2\},\{0,0,0,0\}\}$	0

Continued on next page

Table C.2 – continued from previous page

Representations and vertices	Value
$\{\{11,3,2,11,3,2\},\{0,0,0,0\}\}$	$\frac{4N_c^3-7N_c+6}{N_c^2(N_c+2)(N_c^2-9)(N_c^2-1)^2}$
$\{\{11,4,2,2,4,2\},\{0,0,0,0\}\}$	$\frac{1}{-N_c^4+5N_c^2-4}$
$\{\{11,4,2,2,5,2\},\{0,0,0,0\}\}$	$\frac{3}{N_c^4-5N_c^2+4}$
$\{\{11,4,2,2,6,2\},\{0,0,0,0\}\}$	$-\frac{\sqrt{3}}{(N_c-1)N_c\sqrt{(N_c+3)(N_c^3+N_c^2-4N_c-4)}}$
$\{\{11,4,2,3,4,2\},\{0,0,0,0\}\}$	$-\frac{2}{N_c^5-5N_c^3+4N_c}$
$\{\{11,4,2,3,5,2\},\{0,0,0,0\}\}$	$-\frac{6}{N_c(N_c^5-3N_c^4-5N_c^3+15N_c^2+4N_c-12)}$
$\{\{11,4,2,4,4,2\},\{s,0,0,s\}\}$	$-\frac{2}{N_c^6-14N_c^4+49N_c^2-36}$
$\{\{11,4,2,4,4,2\},\{s,0,0,a\}\}$	$\frac{\sqrt{N_c^2-9(N_c^4-5N_c^2+4)}}{2}$
$\{\{11,4,2,4,4,2\},\{a,0,0,s\}\}$	$-\frac{2}{\sqrt{N_c^2-9(N_c^4-5N_c^2+4)}}$
$\{\{11,4,2,4,4,2\},\{a,0,0,a\}\}$	0
$\{\{11,4,2,4,6,2\},\{s,0,0,0\}\}$	$-\frac{\sqrt{6}}{(N_c-2)N_c(N_c^2-1)\sqrt{N_c^2-N_c-6}}$
$\{\{11,4,2,4,6,2\},\{a,0,0,0\}\}$	$-\frac{\sqrt{6}}{(N_c-2)N_c(N_c^2-1)\sqrt{N_c^2+5N_c+6}}$
$\{\{11,4,2,6,4,2\},\{0,0,0,0\}\}$	$\frac{2}{N_c^5-5N_c^3+4N_c}$
$\{\{11,4,2,6,5,2\},\{0,0,0,0\}\}$	$-\frac{6}{N_c(N_c^5+3N_c^4-5N_c^3-15N_c^2+4N_c+12)}$
$\{\{11,4,2,6,6,2\},\{0,0,0,s\}\}$	$\frac{\sqrt{6}\sqrt{\frac{N_c+4}{N_c+2}}}{N_c(N_c^4+N_c^3-7N_c^2-N_c+6)}$
$\{\{11,4,2,6,6,2\},\{0,0,0,a\}\}$	$-\frac{\sqrt{6}\sqrt{\frac{N_c-2}{N_c^3}}}{N_c^4+N_c^3-7N_c^2-N_c+6}$
$\{\{11,4,2,8,4,2\},\{0,0,0,0\}\}$	$-\frac{4}{N_c(N_c+1)(N_c^4-4N_c^3-N_c^2+16N_c-12)}$
$\{\{11,4,2,9,4,2\},\{0,0,0,0\}\}$	$\frac{4}{(N_c^2-9)(N_c^4-5N_c^2+4)}$
$\{\{11,4,2,11,3,2\},\{0,0,0,0\}\}$	$-\frac{9}{N_c(N_c+2)(N_c^2-9)(N_c^2-1)^2}$
$\{\{11,4,2,11,4,2\},\{0,0,0,0\}\}$	$\frac{4N_c^2-31}{(N_c^2-9)(N_c^2-4)(N_c^2-1)^2}$
$\{\{11,5,2,2,4,2\},\{0,0,0,0\}\}$	$\frac{3}{N_c^4-5N_c^2+4}$
$\{\{11,5,2,2,6,2\},\{0,0,0,0\}\}$	$-\frac{\sqrt{3}}{(N_c-1)N_c\sqrt{(N_c+3)(N_c^3+N_c^2-4N_c-4)}}$
$\{\{11,5,2,3,4,2\},\{0,0,0,0\}\}$	$-\frac{6}{N_c(N_c^5-3N_c^4-5N_c^3+15N_c^2+4N_c-12)}$
$\{\{11,5,2,5,6,2\},\{s,0,0,0\}\}$	$-\frac{\sqrt{6}}{(N_c-2)N_c(N_c^2-1)\sqrt{N_c^2-N_c-6}}$
$\{\{11,5,2,5,6,2\},\{a,0,0,0\}\}$	$\frac{\sqrt{6}}{(N_c-2)N_c(N_c^2-1)\sqrt{N_c^2+5N_c+6}}$
$\{\{11,5,2,6,4,2\},\{0,0,0,0\}\}$	$-\frac{6}{N_c(N_c^5+3N_c^4-5N_c^3-15N_c^2+4N_c+12)}$
$\{\{11,5,2,6,6,2\},\{0,0,0,s\}\}$	$\frac{\sqrt{6}\sqrt{\frac{N_c+4}{N_c+2}}}{N_c(N_c^4+N_c^3-7N_c^2-N_c+6)}$
$\{\{11,5,2,6,6,2\},\{0,0,0,a\}\}$	$\frac{\sqrt{6}\sqrt{N_c(N_c^2-3N_c+2)}}{(N_c-2)(N_c-1)^{3/2}N_c^2(N_c^2+4N_c+3)}$
$\{\{11,5,2,11,4,2\},\{0,0,0,0\}\}$	$\frac{9}{(N_c^2-9)(N_c^2-4)(N_c^2-1)^2}$
$\{\{11,6,2,2,6,2\},\{0,0,0,0\}\}$	$\frac{1}{(N_c-1)N_c^2(N_c+3)}$
$\{\{11,6,2,4,6,2\},\{0,0,0,0\}\}$	$\frac{2}{N_c^2(N_c^3-7N_c+6)}$

Continued on next page

Table C.2 – continued from previous page

Representations and vertices	Value
$\{\{11,6,2,6,6,2\},\{s,0,0,s\}\}$	$-\frac{2}{N_c(N_c^4+N_c^3-7N_c^2-N_c+6)}$
$\{\{11,6,2,6,6,2\},\{s,0,0,a\}\}$	0
$\{\{11,6,2,6,6,2\},\{a,0,0,a\}\}$	$\frac{2}{(N_c-1)N_c^2(N_c^2+4N_c+3)}$
$\{\{11,6,2,11,3,2\},\{0,0,0,0\}\}$	$\frac{9}{N_c^2(N_c^2-9)(N_c^2-1)^2}$
$\{\{11,6,2,11,4,2\},\{0,0,0,0\}\}$	$-\frac{9}{(N_c-2)N_c(N_c^2-9)(N_c^2-1)^2}$
$\{\{11,6,2,11,6,2\},\{0,0,0,0\}\}$	$\frac{4N_c^3-7N_c-6}{(N_c-2)N_c^2(N_c^2-9)(N_c^2-1)^2}$
$\{\{12,4,2,2,4,2\},\{0,0,0,0\}\}$	$-\frac{2}{N_c^4-5N_c^2+4}$
$\{\{12,4,2,2,6,2\},\{0,0,0,0\}\}$	$\frac{2\sqrt{3}}{(N_c-1)N_c\sqrt{(N_c^2-4)(N_c^2+4N_c+3)}}$
$\{\{12,4,2,3,4,2\},\{0,0,0,0\}\}$	$-\frac{4}{N_c^5-5N_c^3+4N_c}$
$\{\{12,4,2,4,4,2\},\{s,0,0,s\}\}$	$\frac{3N_c-1}{N_c(N_c+3)(N_c^4-5N_c^2+4)}$
$\{\{12,4,2,4,4,2\},\{s,0,0,a\}\}$	$\frac{\sqrt{N_c^2-9}}{N_c(N_c+3)(N_c^4-5N_c^2+4)}$
$\{\{12,4,2,4,4,2\},\{a,0,0,s\}\}$	$-\frac{\sqrt{N_c^2-9}}{N_c(N_c+3)(N_c^4-5N_c^2+4)}$
$\{\{12,4,2,4,4,2\},\{a,0,0,a\}\}$	$-\frac{3}{N_c^5-5N_c^3+4N_c}$
$\{\{12,4,2,4,6,2\},\{s,0,0,0\}\}$	$-\frac{\sqrt{6}(N_c+2)\sqrt{N_c^4-5N_c^3+5N_c^2+5N_c-6}}{N_c(N_c+3)(N_c^4-5N_c^2+4)^{3/2}}$
$\{\{12,4,2,4,6,2\},\{a,0,0,0\}\}$	$-\frac{\sqrt{6}\sqrt{\frac{N_c+3}{N_c+2}}}{N_c^5+N_c^4-7N_c^3-N_c^2+6N_c}$
$\{\{12,4,2,6,4,2\},\{0,0,0,0\}\}$	$-\frac{2}{(N_c+1)(N_c^2-4)(N_c^2+2N_c-3)}$
$\{\{12,4,2,6,6,2\},\{0,0,0,s\}\}$	$\frac{\sqrt{6}\sqrt{N_c^2+6N_c+8}}{N_c(N_c^2+2N_c-3)(N_c^3+7N_c^2+14N_c+8)}$
$\{\{12,4,2,6,6,2\},\{0,0,0,a\}\}$	$-\frac{\sqrt{6}\sqrt{\frac{N_c-2}{N_c^3}}}{N_c^4+N_c^3-7N_c^2-N_c+6}$
$\{\{12,4,2,8,4,2\},\{0,0,0,0\}\}$	$\frac{4}{N_c^6-5N_c^4+4N_c^2}$
$\{\{12,4,2,9,4,2\},\{0,0,0,0\}\}$	$-\frac{4(N_c-3)}{N_c(N_c^6-14N_c^4+49N_c^2-36)}$
$\{\{12,4,2,11,4,2\},\{0,0,0,0\}\}$	$-\frac{4}{N_c^6+3N_c^5-5N_c^4-15N_c^3+4N_c^2+12N_c}$
$\{\{12,4,2,11,6,2\},\{0,0,0,0\}\}$	0
$\{\{12,4,2,12,4,2\},\{0,0,0,0\}\}$	$\frac{4N_c^2+4N_c+6}{N_c^2(N_c^2+4N_c+3)(N_c^4+3N_c^3-8N_c^2-12N_c+16)}$
$\{\{12,6,2,2,4,2\},\{0,0,0,0\}\}$	$\frac{2\sqrt{3}}{(N_c-1)N_c\sqrt{(N_c^2-4)(N_c^2+4N_c+3)}}$
$\{\{12,6,2,2,6,2\},\{0,0,0,0\}\}$	$\frac{2}{(N_c-1)N_c^2(N_c+3)}$
$\{\{12,6,2,4,4,2\},\{0,0,0,s\}\}$	$-\frac{\sqrt{6}(N_c+2)\sqrt{N_c^4-5N_c^3+5N_c^2+5N_c-6}}{N_c(N_c+3)(N_c^4-5N_c^2+4)^{3/2}}$
$\{\{12,6,2,4,4,2\},\{0,0,0,a\}\}$	$\frac{\sqrt{6}(N_c+2)\sqrt{N_c^4+N_c^3-7N_c^2-N_c+6}}{N_c(N_c+3)(N_c^4-5N_c^2+4)^{3/2}}$
$\{\{12,6,2,4,6,2\},\{0,0,0,0\}\}$	$-\frac{2}{N_c^2(N_c+3)(N_c^2-1)}$
$\{\{12,6,2,5,6,2\},\{0,0,0,0\}\}$	$\frac{4}{N_c^2(N_c^3-7N_c+6)}$
$\{\{12,6,2,6,4,2\},\{s,0,0,0\}\}$	$\frac{\sqrt{6}\sqrt{N_c^2+6N_c+8}}{N_c(N_c^2+2N_c-3)(N_c^3+7N_c^2+14N_c+8)}$

Continued on next page

Table C.2 – continued from previous page

Representations and vertices	Value
$\{\{12,6,2,6,4,2\},\{a,0,0,0\}\}$	$\frac{\sqrt{6}\sqrt{\frac{N_c-2}{N_c^3}}}{N_c^4+N_c^3-7N_c^2-N_c+6}$
$\{\{12,6,2,6,6,2\},\{s,0,0,s\}\}$	$-\frac{N_c+10}{N_c^6+5N_c^5-3N_c^4-29N_c^3+2N_c^2+24N_c}$
$\{\{12,6,2,6,6,2\},\{s,0,0,a\}\}$	$-\frac{3\sqrt{N_c(N_c+2)}(N_c^4+4N_c^3-7N_c^2-22N_c+24)}{N_c^2(N_c+1)(N_c^2+2N_c-8)(N_c^2+2N_c-3)^{3/2}}$
$\{\{12,6,2,6,6,2\},\{a,0,0,s\}\}$	$\frac{3\sqrt{N_c(N_c+2)}(N_c^4+4N_c^3-7N_c^2-22N_c+24)}{N_c^2(N_c+1)(N_c^2+2N_c-8)(N_c^2+2N_c-3)^{3/2}}$
$\{\{12,6,2,6,6,2\},\{a,0,0,a\}\}$	$\frac{1}{N_c^2(N_c+1)(N_c^2+2N_c-3)}$
$\{\{12,6,2,11,4,2\},\{0,0,0,0\}\}$	0
$\{\{12,6,2,11,6,2\},\{0,0,0,0\}\}$	$-\frac{4}{N_c^2(N_c+1)(N_c^3-7N_c+6)}$
$\{\{12,6,2,12,4,2\},\{0,0,0,0\}\}$	$-\frac{18}{N_c^2(N_c^2+4N_c+3)(N_c^4+3N_c^3-8N_c^2-12N_c+16)}$
$\{\{12,6,2,12,6,2\},\{0,0,0,0\}\}$	$\frac{2(2N_c^2+6N_c-5)}{N_c^2(N_c+1)(N_c+3)(N_c^4+3N_c^3-8N_c^2-12N_c+16)}$
$\{\{14,6,2,12,6,2\},\{0,0,0,0\}\}$	$\frac{4}{N_c^2(N_c+3)(N_c^3+N_c^2-10N_c+8)}$
$\{\{15,6,2,2,6,2\},\{0,0,0,0\}\}$	$\frac{4}{(N_c-1)N_c^2(N_c+3)}$
$\{\{15,6,2,4,6,2\},\{0,0,0,0\}\}$	$-\frac{4}{N_c^2(N_c+3)(N_c^2-1)}$
$\{\{15,6,2,6,6,2\},\{s,0,0,s\}\}$	$\frac{4}{N_c(N_c+1)(N_c+4)(N_c^2+2N_c-3)}$
$\{\{15,6,2,6,6,2\},\{s,0,0,a\}\}$	0
$\{\{15,6,2,6,6,2\},\{a,0,0,a\}\}$	$-\frac{4}{N_c^2(N_c+1)(N_c^2+2N_c-3)}$
$\{\{15,6,2,11,6,2\},\{0,0,0,0\}\}$	$\frac{4}{N_c^2(N_c+1)^2(N_c^2+2N_c-3)}$
$\{\{15,6,2,12,6,2\},\{0,0,0,0\}\}$	$-\frac{4}{(N_c-1)N_c^2(N_c+3)(N_c^2+5N_c+4)}$
$\{\{15,6,2,15,6,2\},\{0,0,0,0\}\}$	$\frac{4(N_c^2+3N_c+8)}{N_c^2(N_c+1)^2(N_c+3)(N_c+4)(N_c^2+4N_c-5)}$

References

- [1] J. E. Paton and H.-M. Chan, *Generalized veneziano model with isospin*, *Nucl.Phys.* **B10** (1969) 516–520.
- [2] P. Dittner, *Invariant tensors in $SU(3)$. II.*, *Commun.Math.Phys.* **27** (1972) 44–52.
- [3] P. Cvitanović, *Group theory for Feynman diagrams in non-Abelian gauge theories*, *Phys.Rev.* **D14** (1976) 1536–1553.
- [4] P. Cvitanović, P. Lauwers, and P. Scharbach, *Gauge Invariance Structure of Quantum Chromodynamics*, *Nucl.Phys.* **B186** (1981) 165.
- [5] M. L. Mangano, S. J. Parke, and Z. Xu, *Duality and Multi - Gluon Scattering*, *Nucl.Phys.* **B298** (1988) 653.
- [6] M. L. Mangano, *The Color Structure of Gluon Emission*, *Nucl.Phys.* **B309** (1988) 461.
- [7] Z. Nagy and D. E. Soper, *Parton showers with quantum interference*, *JHEP* **0709** (2007) 114, [[arXiv:0706.0017](#)].
- [8] M. Sjö Dahl, *Color structure for soft gluon resummation: A General recipe*, *JHEP* **0909** (2009) 087, [[arXiv:0906.1121](#)].
- [9] S. Platzer and M. Sjö Dahl, *Subleading N_c improved Parton Showers*, *JHEP* **1207** (2012) 042, [[arXiv:1201.0260](#)].
- [10] F. Maltoni, K. Paul, T. Stelzer, and S. Willenbrock, *Color flow decomposition of QCD amplitudes*, *Phys.Rev.* **D67** (2003) 014026, [[hep-ph/0209271](#)].
- [11] S. Keppeler and M. Sjö Dahl, *Orthogonal multiplet bases in $SU(N_c)$ color space*, *JHEP* **1209** (2012) 124, [[arXiv:1207.0609](#)].
- [12] M. G. Sotiropoulos and G. F. Sterman, *Color exchange in near forward hard elastic scattering*, *Nucl.Phys.* **B419** (1994) 59–76, [[hep-ph/9310279](#)].
- [13] N. Kidonakis, G. Oderda, and G. F. Sterman, *Evolution of color exchange in QCD hard scattering*, *Nucl.Phys.* **B531** (1998) 365–402, [[hep-ph/9803241](#)].
- [14] Y. Dokshitzer and G. Marchesini, *Soft gluons at large angles in hadron collisions*, *JHEP* **0601** (2006) 007, [[hep-ph/0509078](#)].
- [15] A. Kyrieleis and M. Seymour, *The Colour evolution of the process $q q \rightarrow q q g$* , *JHEP* **0601** (2006) 085, [[hep-ph/0510089](#)].
- [16] M. Sjö Dahl, *Color evolution of $2 \rightarrow 3$ processes*, *JHEP* **0812** (2008) 083, [[arXiv:0807.0555](#)].
- [17] M. Beneke, P. Falgari, and C. Schwinn, *Soft radiation in heavy-particle pair production: All-order colour structure and two-loop anomalous dimension*, *Nucl.Phys.* **B828** (2010) 69–101, [[arXiv:0907.1443](#)].
- [18] P. Cvitanović, *Group Theory: Birdtracks, Lie's, and Exceptional Groups*. Princeton University Press, 2008.
- [19] S. Sternberg, *Group Theory and Physics*. Cambridge University Press, 1995.
- [20] H. Georgi, *Lie Algebras in Particle Physics*. Perseus Books, 1999.

- [21] S. R. G.H. Hardy, *Une formule asymptotique pour le nombre des partitions de n* , *Comptes rendus hebdomadaires des séances de l'Académie des Sciences*. **164** (1917) 35–38.
- [22] A. Yutsis, I. Levinson, and V. Vanagas, *Theory of angular momentum*. Isreal Program for Scientific Translations, 1962.
- [23] D. S. Bernstein, *Matrix Mathematics*. Princeton University Press, 2009.
- [24] M. Sjødahl, *ColorMath - A package for color summed calculations in $SU(N_c)$* , *Eur.Phys.J.* **C73** (2013) 2310, [[arXiv:1211.2099](#)].
- [25] Y.-J. Du, M. Sjødahl, and J. Thoren, *Work in preparation*, .